Environmental pollution effects on insulators of high voltage overhead transmission line for locomotives

By

Trevor Teron Mabunda

214526813

A dissertation submitted in partial fulfillment of the requirements for the degree

Of

Master of Science in Electrical Engineering

College of Agriculture, Engineering and Science, University of KwaZulu-Natal

2019

Supervisor: Dr. A. Saha

As the candidate's Supervisor I agree/do not agree to the submission of this thesis. The supervisor must sign all copies after deleting which is not applicable

Signed: _____

Dr. A Saha

I Trevor Teron Mabunda declare that

1. The research reported in this thesis, except where otherwise indicated, and is my original research.
2. This thesis has not been submitted for any degree or examination at any other university.
3. This thesis does not contain other persons' data, pictures, graphs or other information, unless specifically acknowledged as being sourced from other persons.
4. This thesis does not contain other persons' writing, unless specifically acknowledged as being sourced from other researchers. Where other written sources have been quoted, then:

a) Their words have been re-written but the general information attributed to them has been referenced
b) Where their exact words have been used, then their writing has been placed in italics and inside quotation marks, and referenced.

5. This thesis does not contain text, graphics or tables copied and pasted from the Internet, unless specifically acknowledged, and the source being detailed in the thesis and in the References sections.

Signed: _____

Trevor Teron Mabunda

ACKNOWLEDGEMENTS

ABSTRACT

The primary focus of this research is to report thoroughly on the addressed key questions of the proposal and to successfully compile a simulation based on environmental pollution effects on insulators of high voltage overhead transmission line for locomotives. The simulation design is done on FEMM, which provides useful models for solving electromagnetic problems, which will assist to compile a suitable insulation model design with results that can be interpreted in detail. This report includes the theoretical background of a high voltage insulator for different materials with different sizes and shapes affected by different environmental conditions. Ceramic insulators appear to be extremely susceptible. Polymeric insulators specially of silicone-rubber have achieved better performance under polluted states and have found increasing usage. The feasibility study conducted shows that the simulation design is feasible and transparent. The IEEE and ScienceDirect publications are the suitable sources that are used to conduct the literature review. The method used to collect data and information or research strategy which summarizes the way in which research will be undertaken is conduced. Furthermore, the preliminary research results and analysis evolve after investigating and analyzing the electric field distribution of a polymeric insulator, which is commonly used on high voltage overhead transmission line for locomotives when it is dry and when a water drop is applied with and without a corona ring. In the three cases investigated, the first case is when the insulator was dry, the second case is when water droplets reside as a discrete droplet on a polymeric insulator made of a silicon rubber material and the third case is when the corona ring is added, simulation was executed for both typical and optimized insulators. It was found that the presents of water droplets on the insulators either due to rain, fog, etc. leads to electric field enhancement causing partial discharge and dry arc which ultimately results in complete flashover. The current work has resulted in a simple model to estimate the flashover voltage of a polymeric insulator under contaminated states. To ensure reliability, simulation results are compared with existing work carried in the past.

Table of Contents

List of figures

List of Tables

List of Abbreviations

A	Ampere
AC	Alternating Current
ESSD	Equivalent Salt Deposit Density
FRP	Fiberglass Reinforced Polymer
DC	Direct Current
FEMM	Finite Element Method Magnetics
FOV	Flashover or Breakdown Voltage
HVAC	High Voltage Alternating Current
HV	High Voltage
HVDC	High Voltage Direct Current
IEC	International Electrotechnical Commission
LI	Lightning Impulse
IEEE	Institute of Electrical and Electronics Engineers
NSDD	Non-soluble Deposit Density
SDD	Soluble Deposit Density
LRD	Loop Relay Degree
SiR	Silicone Rubber
kV	Kilo Volt
kW	Kilo Watts
LV	Low Voltage
MV	Medium Voltage
MVA	Mega Volts Ampere
MW	Mega Watts
OHTL	Overhead Transmission Line
UV	Ultra-violet
KVA	Kilo-Volt Ampere
E	Electric field
F	Electrostatic Force
σ	Conductivity
UPCM	Unified Protection Coordination Model
HVTL	High Voltage Transmission Line
V	Voltage
W	Watts

Chapter 1
Introduction

1.1 Research work

The HVTL power system is used to distribute electrical energy, generated from a DC or AC power supply. The electrical energy must be separated or isolated to where it is not required through insulation. Different types of insulators are used to provide insulation for a rated transmission line. However, there are external factors that may affect the insulator performance. Additionally, the external factors can include molecules, chemicals, substances or moisture. These extern factors are called pollutants or contaminants: which are not desirable because they have a negative impact on the insulator performance.

Insulators operating under different uncontrolled external conditions and different voltage levels can be affected differently, which are subjected to an unpredictable risk of flashover. Moreover, flashovers induced by contaminants affect normal operations of electric power systems due to insulation failure. Different approaches were taken to mitigate flashover caused by contaminants. However, insulation design has improved with time, improvements done may include shape, size, material, etc.

1.2 Background

High Voltage insulators have been used extensively to provide insulation for electrical systems and to provide mechanical support for different transmission lines. AC power supply has been preferably used for transmitting and distribution electrical energy over a century, the transmitted electrical energy has been used in low voltage distribution to supply electrical power to commercial, residential and industrial loads. The low voltage and high voltage systems required insulation for safe operation.

The insulator is the main equipment in power systems that do not conduct electricity and responsible for tolerating conductor weight. Pollution introduces contaminants into the environment to cause undesired changes in the insulator. More recently, new problems related to insulators degradation and failure such as brittle fracture have been reported, and models in which water droplet corona plays a role were proposed [1].

However, there were different challenges and limitations of utilizing AC distribution or transmission systems. The challenges include the capacitive power loses, distance limitations as well as the impracticality of connecting two AC power networks directly of different frequencies from different supplies. Insulators could provide the isolation of an unsynchronized AC transmission system and break the system into sections to avoid distance limitation and reduce capacitive power losses.

Furthermore, various technical and technological studies have been previously conducted to define the physical properties of HVDC insulators. However, practical aspects that may include the insulator resistivity and permittivity for different electrical characteristics where not clearly defined in the introduction of composite insulators. HVDC transmission systems are expected to expand to enhance the efficiency of electrical power distribution, although rectification can be more complex and expensive.

1.3 Motivation

During exposure to the high voltage overhead transmission line equipment at Transnet: it was discovered that there was an insulation failure near an industrial area. The industry was emitting chemicals (carbon-dioxide and Sulphate), which were causing the insulators to conduct when there was moisture in the air. The emitted chemicals would cause the insulators to flashover and cause the substation to malfunction with burnt electrical components. Solutions to mitigate or to solve the problem in the system were not proposed. Therefore: new design specifications and the improved system must be implemented with a better understanding of high voltage insulators. This study is important because there had been failures in the electric locomotive industries due to the threat caused by harmful pollutants that include fog, dust, condensation, moisture, absorption and reactive gases emitted from other industries. One cannot tell how much pollution can cause corona or insulation to flashover. These interrupt the running of businesses in most of the industries.

1.4 Research questions

Investigating under the proposed topic it should be well known that:

- Why outdoor insulation is important and
- Why it should not only have high dielectric strength but should be capable of performing under harsh environmental conditions.
- Why a current path is created for the current flow between the live conductor and earth conductor to cause corrosion? In addition, how to determine the type of material suitable to be used for different environmental conditions?
- What can be done to mitigate the effects that cause flashover to occur, to reduce corona and to control electric fields (in AC transmission line)?
- What are the characteristics related to different pollutants on an insulator to cause flashover and how flashover occurs depending on the type of pollutants?

1.5 Thesis feasibility study

Through reviewing the work done from the previous literature, it can be agreed that the available literature can assist to successfully compile the proposed research study. The insulators are widely used, and they are being continuously upgraded to keep up with the latest systems. Therefore, the continuous increase in the usage of insulators grants an opportunity for performance improvements under different conditions to reduce flashover. This can be achieved by utilizing the available resources to improve the physical and technological design of the electrical insulators.

1.6 Thesis aim and objective

The aim of this research study was to study and understand the proposed topic and to develop a simulation model that would both be the representable and replacement of the HVAC and HVDC outdoor insulators utilized on the overhead transmission line for locomotives. The research objectives were as follows:

- To simulate and discuss the behavior of AC and DC conductors when exposed to the environment pollution levels
- To simulate and discuss the electrical performance under different polluted conditions as well as under overvoltage conditions
- To compare simulated results with the types of flashovers by SANS 60815 Standards and what precautions must be taken to prevent failures

1.7 Problem statement

Flashover of polluted high voltage insulators is a major problem for the operation of power lines, which are most likely to be affected quickly [3]. Effects may lead to significant failures that may include hook-ups, corrosion, etc. Thereby, the high voltage insulator must be designed for the loads imposed on it by the Over-Head Transmission Line (OHTL).

1.8 Outline of the dissertation

The dissertation of this report is divided into five main chapters:

Chapter 2 provides the literature review of the types of high voltage insulators used in the overhead transmission line of the locomotive. This chapter discusses the detailed properties of each insulator and how those properties contribute to insulator performance. The general insulator performance that includes failure modes and various factors that have a negative impact on the insulator performance are discussed as well.

Chapter 3 illustrates the experimental system set-up and procedure utilized to achieve comprehensive results through simulation. Furthermore, detailed quantitative properties are discussed for each simulated insulator model developed to assist with a better understanding of the electric fields and voltage distribution.

Chapter 4 presents the preliminary results and analysis with the simulated insulator models illustrating a detailed qualitative view of the behavior of the electric field on various conditions. The outcomes are to be compared to previously published results.

Chapter 5 presents the main research results and analysis discussion, backed up by theories from previously done studies. The numeric results are recorded through MATLAB simulation for different voltage levels and tabulated. The results are presented graphically from the numerical values obtained through simulations.

Chapter 6 presents conclusions and recommendations that are obtained from the finds and propositions from future work.

Chapter 2
Literature review

The Literature breakdown evaluation of the two kinds of insulators employed within this research study is presented in this chapter. The types of materials utilized for the outdoor insulators are crucial, whilst the materials need to have high-quality strength properties. However, should be effective at operating under harsh environmental conditions, such as ultraviolet rays, contamination, and over-voltages over a long period. The topical insulators are classified into ceramic (porcelain and glass) and non-ceramic (polymeric) insulators.

2.1 Flashover theory

Though the study of the process of contamination flashover has been done for many decades at different labs and at outdoor locations across the world, the understanding of the physical process is not complete even now. This can be attributed to the intense complexity involved in the flashover process [1]. Also, the numerous parameters involved in the process of flashover make it even more difficult to understand the process completely. As an example it has been observed in service that flashover voltage depends upon various factors but is not limited to such as, the polarity of voltage, particle size, non-uniform wetting, the size and nature of the pollutant surface conductivity, wind, washing, length, orientation, diameter and profile of the insulator [2].

Various other researchers have proposed alternative models to that of Obenaus. Hampton proposed a theory based on an experiment in which he used a water jet to simulate a contaminated long rod insulator [2]. According to Hampton's theory, flashover voltage was treated primarily as a stability problem. Hampton stated that an unstable situation occurs if there is a current increase when the discharge root is displaced in the direction of flashover. From this he concluded that if the voltage gradient along the discharge was ever to fall below the gradient along the resistive column, then flashover would occur. Subsequently it was mathematically proven by Hesketh that Hampton's two criteria of voltage gradient and current increase were identical only in the case of a long rod insulator [3]].

Obenaus was the first to propose a model for contamination flashover. Obenaus outlined the steps that were required to calculate the flashover voltage [12]. The actual computation was completed by Neumarker who derived an expression that relates flashover voltage and surface conductivity [13]. In this theory flashover process is modeled as a discharge in series with a resistance as shown in appendix A figure 45. Here the discharge represents the arc bridging the dry band, and the resistance represents the un-bridged portion of the insulator. The voltage drop across the resistance is taken as a linear function of current. The equations derived for critical voltage gradient (E_c) and critical current (I_c) are [17-20],

$$E_c = N^{(\frac{1}{a+1})} \times R_p^{(\frac{a}{a+1})} \tag{1}$$

$$I_c = \frac{N^{(\frac{1}{a+1})}}{Rp} \tag{2}$$

where

$R_P \quad = \quad \frac{R_{poln}}{LD, \ Larc}$, uniform surface resistance per unit length of the pollution layer

$N \qquad$ = Reignition constant

$a \qquad$ = Arc equation exponent

$R_{poln} \quad$ = Series resistance of the pollution layer

$LD, \ Larc$ = Leakage distance and arc length respectively.

2.2 Flashover theory in partially contaminated insulators

Apart from the various theories discussed so far regarding a uniformly contaminated insulator, flashover, was observed also in a partially or a non-uniformly contaminated insulator. In many insulator flashovers have taken place without any indication of surface discharge activity. The flashover voltage is much lower than predicted by clean fog. High non-uniform voltage distribution is believed to trigger streamer discharges. Some significant observations in this type of flashover termed as sudden flashover are [4, 5]:

- In streamer discharge FOV is non-linear to leakage distance.
- The high resistance region near the HV end causes higher field intensification
- Insulators with smaller shed spacing suffered a significant reduction in
- performance as smaller shed spacing may itself aid an arc to jump
- In contrast to wholly contaminated insulators the path of the arc is essentially
- through air instead of following the leakage distance path
- Hanging water droplets due to rain may substantially reduce dielectric strength
- between sheds
- Complete shed bridging due to water bridging the gap
- Ratio of the resistance/unit length of wet region to dry region is a key parameter
- for prediction

Some possible solutions that are sought of for this problem include but are not limited to:

- Insulator shapes are to be modified with the aim of an improved contamination
- Performance improvement of insulator materials improves the performance (NCI better than ceramic)
- Increase in shed spacing as typically observed in NCI

The properties of polymer insulators tend to change with time because of longtime exposure to UV (Ultraviolet) rays from sunlight, temperature, mechanical loads and electrical discharges in the form of arcing or corona. Such a reduction in the electrical and mechanical properties is termed aging. The silicone rubber insulators tend to lose one of their most important properties of hydrophobicity when they are continually subjected to various extreme levels of environmental factors [6]. The various characteristics of the insulators can be evaluated by the records obtained from service. Though the records from the field are of immense value, they are difficult to obtain and may take a long period of time before their validity can be proved [6]. According to previously done studies, laboratory tests results are increasingly used to evaluate the various performance characteristics of the insulators to correlate with actual field conditions.

Surface resistance generally reflects multivariable, which are typically the type of material, wetting rate, ESDD and the recovery characteristic. The surface resistance of the insulator that has recovered is different from the surface resistance of the un-recovered insulator particularly for the silicone rubber type. Apart from these, surface resistance can be used to assess the aging of the insulating materials [4]. Aging of insulating materials can be defined according to IEC and IEEE standards, as the 'occurrence of irreversible deleterious changes that critically affect performance and shorten useful life.' Aging is a complicated process. Aging would lead to increased leakage current and subsequent flashover of insulators during wet and contaminated conditions. Quantifying and comparing aging in non – ceramic insulators is not a simple task. As aging leads to increased leakage current, it can be assumed that surface resistance measurements can be used as indicators to quantify and compare aging in case of NCI [4].

2.3 Porcelain Insulators

Porcelain insulators have a smooth coating to lose water. The insulators are composed of quartz, alumina or clay together with feldspar; some are produced with a high quantity of alumina to meet high mechanical strength standards [1]. Porcelain contains a dielectric strength of approximately 4-10 kV/mm [2]. Porcelain insulators can be created uniquely in distinct to their size and shape but share similar properties be used broadly and frequently. Advantages include that they are impervious to moisture and resistant to ultraviolet rays [3].

Additionally, it is glistening to deliver a smooth coating to directly inhibit the accumulation of contaminants and helps with natural washing [4]. Furthermore, for contaminated conditions the coating forms a layer of contaminants that has the property to resist the flowing current that enhances the practical functionality of the insulator by allowing a continuous current flow that warms the water to also prevent the formation of dry bands and frequent arcing. Also, it is resistant to be damaged through external discharges and features high compressive strength properties [5].

Disadvantages associated with porcelain include that it is brittle and has a low tensile strength which leads to failure and breakage due to thermal impacts of arcs and its hydrophobic characteristics [6]. The profile of the insulator is introduced into the computer software. Where accuracy is required, the mesh density is significantly higher within the regions of the insulators. The attention is dependent on specifying the source of the electric field distribution and its potential.

2.4 Glass Insulators

Glass which is generally produced from toughened glass to get high mechanical durability. Glass is commonly used for cap and pin suspension insulators [7]. Glass insulator has a high dielectric strength: however, they cause condensation when water is trapped in the surface of the plates [4]. Advantages associated with ceramic insulators composed of glass include that it is tolerant of the environmental effects that constitute moisture and ultraviolet radiation [8]. Disadvantages associated with glass is that it has limited mechanical strength, it is prone to shutter, it is most likely to form a current path for leakage current and it is hydrophilic [7, 9].

In the event of a clean glass insulator, the electric fields are uniformly distributed around the surface of the electrode. There is a significantly high electric field density at the electrode with high potential, it decreases to the ground electrode across the leakage distance [4, 10]. The layers with reduced width have more electric field lines radiating from the surface of the insulator. However, the insulator is more rigid when the conductivity of the surface area increases in addition to its width [8].

2.5 Polymeric Insulators

Polymeric insulators are composed of a polymer composite insulator that is created out of a mechanical strong fiberglass center that is included in a plastic casing to safeguard the core from external environmental effects [11]. The material used comprises ethylene propylene diene monomer, silicone rubber ethylene vinyl acetate, epoxy resin, higher density polyethylene, polytetrafluoroethylene [1]. Additionally, the insulators possess the main benefit of having a high tensile strength to weight ratio.

Silicon rubber insulators are divided into three categories based on healing procedure including pressure, temperature and the representatives used. This can be categorized into a high temperature vulcanized, room temperature vulcanized and the silicon rubber in liquid form [4]. Silicon rubber offers the benefit of hydrophobic properties, which lacks uniform wetting and makes the material less susceptible to discharges [12]. The hydrophobicity is directly credited to the existence of low molecular weight polydimethylsiloxane molecules, that permits the expansion of this hydrophobic feature into the contamination coating. Under wetted contaminated

states, leakage current doesn't flow [13]. The shed profile has a significant role in the pollution performance of the insulator and should be made or chosen according to the environmental requirements [12].

The properties of a clean polymeric insulator allow the voltage supply to be uniformly distributed and gradually decrease from the high voltage end to the low voltage end. Electric fields move toward the link between the metallic and insulating material due to the properties of conductivity of the metal end of the insulator. Furthermore, silicon rubber has high chemical stability and heat resistance to provide better electrical insulation. Additionally, the silicon rubber has high durability that allows better elasticity and high withstand compressibility as well as excellent resistance during cold temperatures.

2.6 Electrical Performance of Insulators
Electrical performance can be achieved when the insulator can withstand the power frequency voltage under dry, wet and contaminated states in addition to under and over-voltage requirement. Furthermore, under dry and wet power frequency flashover. The insulator is required to function at the nominal U_n and maximum U_m operating voltage for an elongated period in wet and dry states [6]. The arc space decides the flashover voltage [14]. The insulator must resist both lightning urge over-voltage and the switching impulse over-voltage [6]. The contamination flashover is a complex process for both ceramic and non-ceramic insulators and can be divided into type A and type B flashovers.

2.7 Pollution Flashover on insulators
According to SANS 60815, type A flashover process is divided into six phases which applies only to the hydrophilic insulators. Pollution flashover begins on the first phase when the insulator is coated by various methods with a coating of contamination, the second phase is when the outside of the insulator becomes wetted through rain, fog absorption, condensation, and so on to induce the contaminants to create an electrolytic coating layer, although not enough to wash the contamination layer away, the third phase is when the surface leakage currents stream inducing heat and also the parts of the contamination coating with the greatest current density dry to form dry-bands [15, 12].

Furthermore, the fourth phase is when the dry-bands interrupts the leakage current, the fifth phase occurs when the live to ground voltage strikes over the dry-bands and induces current around the dry-bands that are electrically in series with the contamination layer, the final phase occurs when the surface is progressively decreasing the resistance and increasing the leakage current until flashover occurs for low resistance, the arcs become sustained and stretch across [15, 13]. Moreover, type B includes significant conductivity fog that occurs and causes temporal flashovers. Also, bird streamers alter the electric industry of the gap to cause flashovers and difficulties in the environment. In this situation, towers are safeguarded to prevent birds from perching above insulators [12].

For the contaminated insulator, the voltage distribution differs, a large part of voltage is shared with the sheds over the higher voltage side; the voltage can be too high in magnitude towards the low voltage side of the insulator. It can be observed that pollutants have the impact of increasing voltage magnitude across the insulator surface. For a polluted polymeric insulator, the electric field strength tends to be raised by the contaminants. The field is more concentrated in the metallic fittings. At the low voltage end, electric field lines are very close, indicating high electric field strength. Electric field density is low on the high voltage end for the polluted insulator.

2.8 Creepage distance in Insulators

However, even the creepage distance is linked to the length of the current path along the insulator. The longer the creepage the higher the resistance of the contamination layer [16]. The role of the material and the shed will be all crucial to reach the required creepage [17]. SANS 60815 defines the unified specific creepage distance for different levels of pollution. Although it has been revealed that the performance of the hydrophobic insulators allows for a decrease in the creepage, it is not recommended due to the aging of polymers due to ultraviolet radiation and corona [16]. The performance of insulators can be tested with a salt fog test and a clean fog test [18].

2.9 Pollution with Corona Flashover

Due to the physical nature of the insulator, corona will be present. The secondary services and products of corona, for example, ultraviolet radiation, ozone, acids at the presence of moisture, also might get a result of polymer insulators [19]. Corona rings are used on high voltage electric power transmission lines of insulator and switching [20]. Corona rings have the properties to control both the electric field and reduce corona.

Corona rings are primarily installed to control the electric field distributed on the end fittings of the insulator under high voltage distribution and reduce corona to minimize insulation failure, which leads to flashover [21]. Thus, considering a wet polymeric insulator without a corona ring, the electric field distribution on the insulator when a single water drop is placed on the insulator cover. The spikes signify the enhancement of the electric field intensity [22]. Comparatively, a wet polymeric insulator with a corona ring discharges a flow of current from the electrode to the [21].

Corona at the initial voltage can be increased by utilizing a standard treatment, like a semiconductor coating, high voltage coating or a corona dope [23]. Additionally, void-free solids that are precisely prepared. Test methods may include, laboratory corona ring (small corona ring), test lines, outdoor corona ring, and operational AC and DC transmission lines [8]. This approach involves providing enough voltage involving the conductor bundle and the rings to generate a high counter surface electrical field. The tests can be done on AC and DC voltages.

The most important objective to be considered when employing this way is the fact that the appearance of the corona ring must have an adequate margin between the breakdown and the corona onset voltage [23, 24]. The advantage of the ring setup is the surface of the electric field distribution that could be determined accurately, the advantage is that it is utilized to find the effectiveness of the corona, which are the corona losses [24]. Operating lines are utilized for the determination of just the corona losses of overhead transmission lines for a locomotive configuration.

The corona ring distributes the electric field gradient and lower its maximum values below the corona threshold and thus preventing corona discharge, which leads to undesired power losses [14, 20]. The behavior of the electric field between the ring and the conductor is illustrated in chapter four. The contaminants are trapped in the insulator shreds forming an electrolytic layer that significantly influences the voltage and electric field distribution. The electrolytic layer conducts from the high voltage side along with the shreds towards the low voltage side of the insulator.

Flashover is directly dependent on the level of the contaminant. Also, fewer contaminants lead to less risk of flashover and more contaminants mean a larger electrolytic later which leads to a high risk of flashover and insulation failure. Furthermore, the physical property of a corona ring is that it is smooth round-shaped to allow the distribution of electrical fields or charges across a wide area. Therefore, the potential gradient will be reduced below the critical disruptive magnitude and the maximum disruptive magnitude value will be lowered below the corona threshold [21].

2.10 The leakage current on pollution layers

The breakdown voltage of the corona ring for AC and DC voltage can be obtained. For AC flashover, the size and shape of the insulator must be chosen accordingly [25]. Thus, the mathematical equation and simulation models must be used. During the process of flashover, the surge current could exceed the rated current of the selected insulator. According to the study conducted by Steinmetz et *al*: 2008, The break-down of the corona ring is 100 kV for DC voltage and 80 kV for AC voltage. During the DC voltage test, flashover occurs between the conductor and the corona ring on the high voltage side of the insulator [25]. Therefore, the greater magnitudes of all AC present are due to AC capacitive and resistive components present while DC has just the resistive component present.

2.11 Wet and Dry Power Frequency Flashover

The electric field distribution of the polymeric insulator when there is a drop of water in the surface of the insulator and the corona ring placed at the high voltage side. The maximum value of the electric field at the high voltage side of the insulator decreases since the corona ring modifies the shape and direction of the electric field intensity [10, 26]. The electric field distribution of the dry contaminants on the polymeric insulator is distributed along the low voltage side [27].

2.12 Switching and Lightning impulse flashover

The effect of discontinuous non-uniform contamination in the flashover of polluted insulators under Lightning impulse voltage [28]. Due to direct strikes and back-flashover lightning may cause insulation to flashover from both ways. Hence, electric equipment insulation strength with protective devices must be used to protect the insulators. In a high voltage transmission line, the insulation of the equipment needs to be able to withstand voltages greater than that of the protective device. In a typical transmission system, the insulation needs to be capable of resisting the standard operating voltage as well as the requirements of temporary over-voltages, switching over-voltages and lightning over-voltages. There is a statistical nature to over-voltages, and these can be computed through the usage of simulation [7, 29].

The possibility of overvoltage occurring (represented by a probability distribution function or Gaussian distribution curve) can be compared with the possibility of insulation breakdown Signified by a cumulative distribution function to find a probability of failure. All manufactured insulators must be able to withstand the basic insulation level, where the rated withstand voltage for insulation expressed as a peak value of the standard lightning impulse under standard atmospheric conditions [28]. Under standard atmospheric conditions, the rated withstand voltage for insulating material expressed as a peak value to its standard switching impulse, which can be referred as a switching insulation level which may change due to the environmental conditions that may affect the insulator performance under both DC and AC power transmission [16].

As a result of increasing voltages, it is critical to upgrade on a high voltage transmission line, devices and insulation materials that can be able to withstand environmental changes. Calculating the electrical field is important in the high voltage technology design Procedure. According to the recommendations done by the International Commission for Non-Ionizing Radiation Protection (ICNIRP), urges that the electric field experienced by the general public to be limited by 5 kV/m also to 10 kV/m for working employees. The World Health Organization (WHO) recommends that the electric fields at power frequency have no noticeable effect on a person, above 15 kV/m an individual experience a mild to intense shock when touching earthed items or climbing from a Car that is exposed to the electric field [23, 28].

Chapter 3
Methodology

This chapter presents the simulated experimental circuits and procedures taken to get results for different insulators exposed in different conditions. Experimental models and tools were employed to simulate the insulator samples with their distinctive properties. The AC generator, flashover detection circuit, HVDC circuit, three-phase flashover detection circuit, and the subsystem circuit configuration were done to obtain feasible results for flashover of contaminated insulators on the OHTL of the locomotive.

3.1 AC generator experimental circuit

To obtain comprehensive test results for HVAC, a 230 kV, 300 kVA, 50 Hz cascaded transformer was used in a simulation model with MATLAB. The HVAC voltage was induced through an insulator under test device which was set with similar properties to the insulator in FEMM [30]. A capacitive voltage divider with an acceptable ratio of 1:5000 was used to obtain the peak flashover voltage value and recorded through a digital oscilloscope tool in figure 3. The simulated circuit diagram is represented in figure 1.
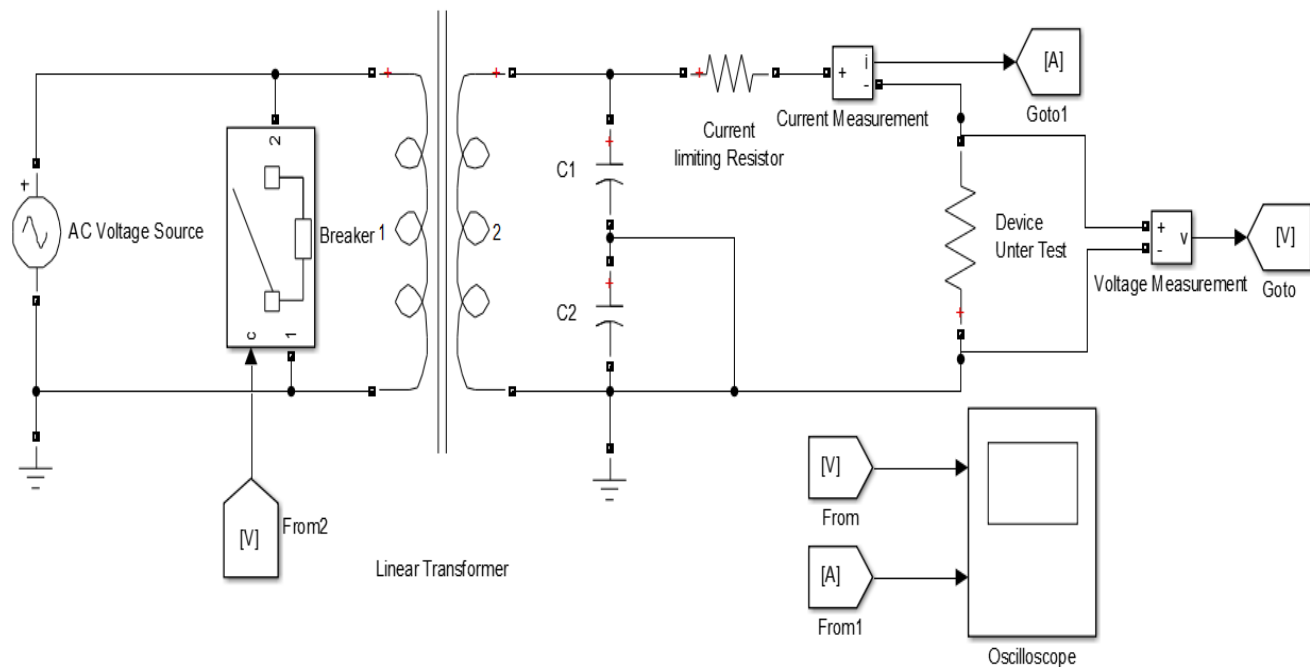
Figure 1: The simulated AC generator schematic circuit

3.2 AC Leakage Current Measurement

The leakage current was measured using an ammeter, where there is a voltage drop through a 4.7 Ω shunt resistor [31]. A small resistance value was considered to make the measuring digital multimeter more sensitive. Furthermore, a 220 V, 40 kA switch was used as a surge protective device to protect the measurement system against surge current or current that may flow backward through the system. The measurement system is connected to the low voltage end of the insulator [32]. According to previously done studies, the total leakage current flows towards the ground connection [31].
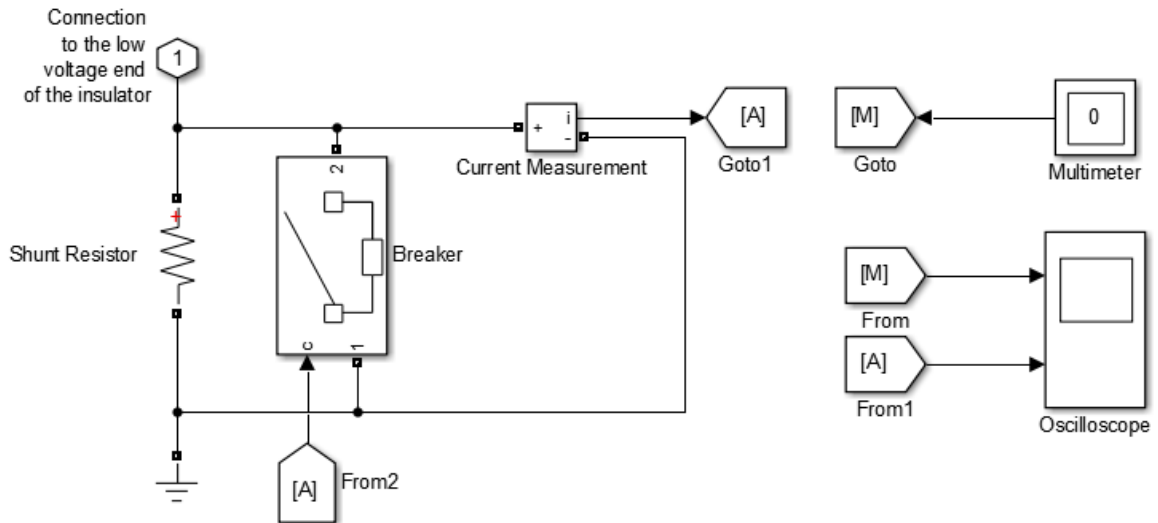
Figure 2: Leakage current measurement system

The current measurement system of the insulator around the corona ring that was used to quantify current is exemplified in figure 2. For the currents to be properly quantified, a shunt resistor (power resistor) is used. The resistor is attached at the center of the corona cage, its function is to allow current to pass through it hence making it possible for the current to be measured across it [33]. The currents that are expected are of low magnitude hence it would be difficult to measure them directly with an ammeter [4, 13]. A voltmeter can be used to measure the voltage across the resistor and the current will be calculated with the Ohm's law formula. The value has been selected primarily based mostly on the lower anticipated currents and to help make the measuring meter more sensitive, this also helps to ensure that accurate outcome of corona present is quantified accurately [4, 13].

3.3 Flashover and Fault detection circuit
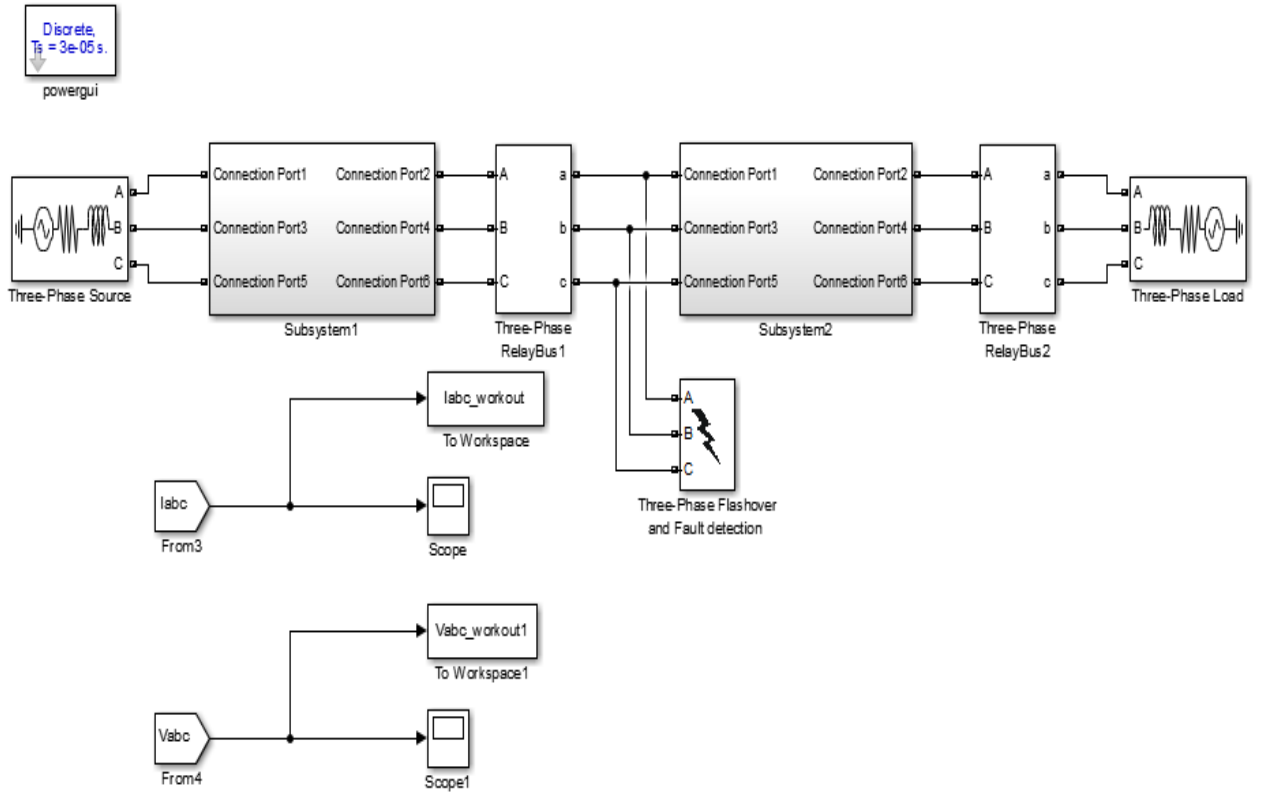
Figure 3: Three-phase flashover detection circuit [34]

The flashover detection circuit has a discrete runtime of 3×10^{-5} seconds to detect instantaneous voltage changes. A variable HVAC source with a frequency of 50 Hz is connected to subsystem 1. The subsystems consist of five individual three-phase PI section lines. The three-phase PI section lines have positive (r_1) and zero-sequence (r_0) resistances of 0.01273 Ohms/km and 0.3864 Ohms/km, a positive (I_1) and zero-sequence (I_0) inductances of 0.9337×10^{-3}H/km and $3\ 4.1264 \times 10^{-3}$ H/km, and a positive (c_1) and zero-sequence (c_0) capacitances of 12.74×10^{-9} F/km and 97.751×10^{-9} F/km. Each transmission line is 30 kilometers long in each three-phase PI section line. The three-phase relay bus1 compares the voltage and current between the subsystems for flashover detection and relay bus 2 protects the load from over-voltages. Relay bus 2 is set to the insulator properties. The two subsystems are shown in figure 4.
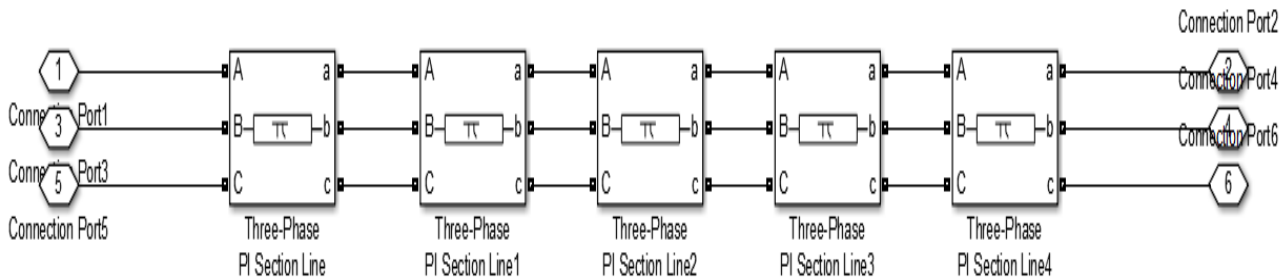
Figure 4: Subsystem circuit configuration [34].

3.4 DC generator experimental circuit
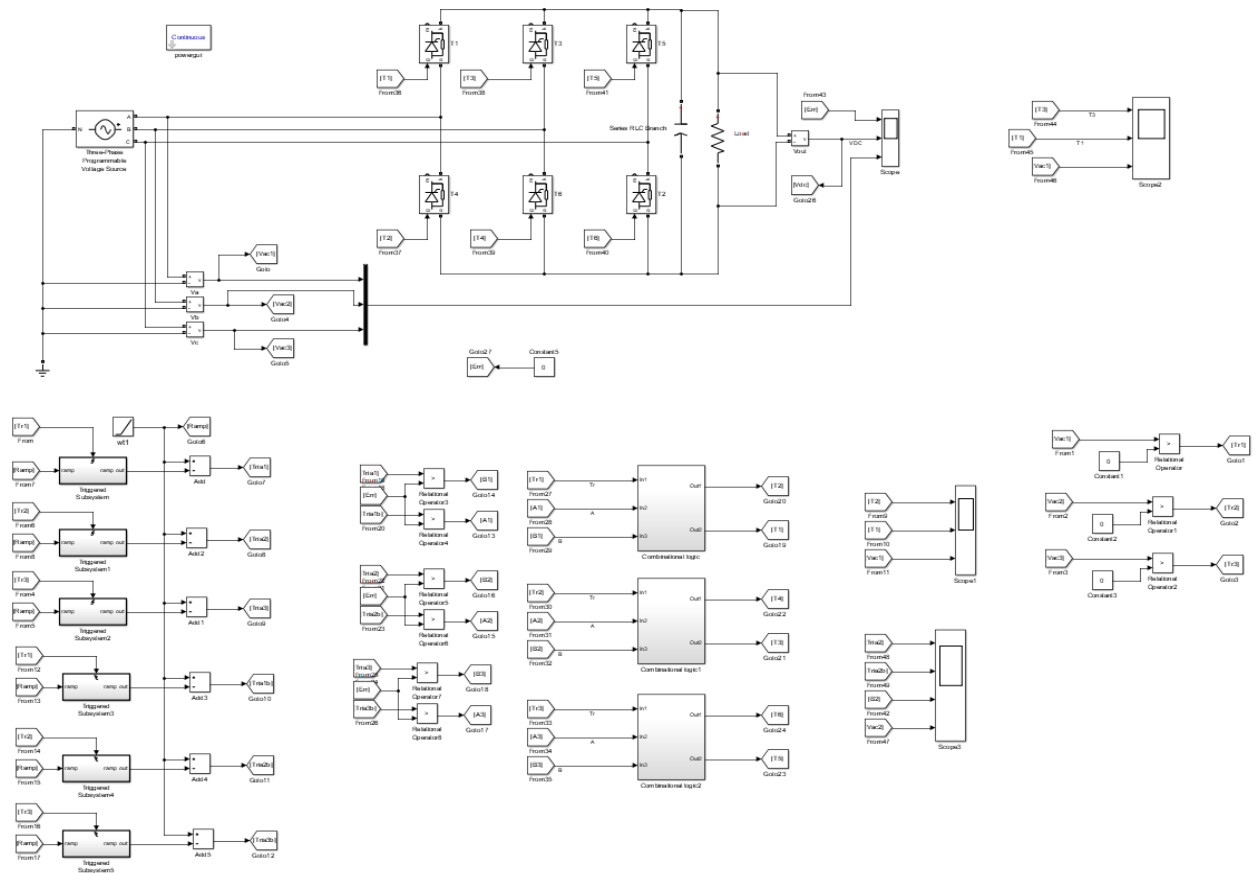
Figure 5:Fully controlled three-phase rectifier

An IGBT fully controlled three-phase rectifier is used to generate HVDC. The HVDC system supply for the OHTL for locomotives is simulated on MATLAB and an insulator model is inserted between the negative and positive terminal of the voltage source. The results are recorded on the tables in appendix B.

The subsystems are used to control the voltage output. Figure 48 in appendix A shows the subsystem that contributes to control the rectifying circuit in figure 5. The subsystem shown in figure 48 of appendix A is responsible to detect Zero crossing points of the input AC signal. The Zero crossing detection is obtained from the input sine wave every time it crosses the zero level; a signal is activated as a logic one by using an appropriate method for the zero crossing. A zero-crossing detector circuit sends a logic high as an interrupt to switch on the IGBT after every 10 ms for a sinusoidal wave oscillating at a frequency of 50 Hz [17].

This interrupt commands the control circuit shown in appendix A figure 49 to switch the IGBTs on/off with different time delays to output the desired voltage magnitude [7]. The generated a delay time is used for trigging the IGBT gate in the range of 1ms to 9 ms to switch voltage levels between minimum and maximum range. The delay angle can be controlled using mathematical model functions, logical diagrams or feedback control system. This process repeats after every 10 ms for rectification of an AC system oscillating at 50 Hz [34].

Synchronization voltage is obtained from line voltage of the IGBT circuit and this configuration ensures that the zero-crossing point from negative to positive of synchronization voltage corresponds proportionally to the phase shift angle ($\alpha = 0$) of the three-phase controlled rectifier circuit. The input frequency of the three sine waves is 50 Hertz meaning and 120 ° apart and alternates at 50 cycles per second.

3.5 Insulator performance

The insulator performance under contamination states can be monitored in several ways. The simulation tests can predict how the contaminated insulators are going to perform under different voltage levels and different contaminant conductivities. Furthermore, since the normal height from ground to OHTL (where the insulator is situated) is $50150\ mm$ for all locomotives, therefore a visual inspection can be done. After flashover has occurred; the glass and porcelain insulators are more likely to break, and the polymeric insulators are more likely to melt the silicon shreds [30]. In addition, a performance test can be carried out at ambient temperature to ensure the insulators meets its specified requirement.

The performance tests should be done but excluding voltage supply interruption. This type of test must include DC supplied equipment; tests must be performed to prove correct functioning of contaminated insulators to prove correct functioning at nominal supply voltage and at the specified upper and lower limits. Considering the AC supplied equipment, tests must be performed to prove correct functioning at nominal voltage and frequency and the upper and lower limits of voltage and frequency the insulator under test must be monitored throughout the test to ensure accurate results [6]. The tests must be carried ten times for each insulator type subjected in dry and wet contaminants tests.

The insulators heat up due to the electric fields around it; thus, the insulator's thermal capacity, thus according to IEC 60068-3-7 a cooling test must be conducted. To achieve thermal stabilization of the insulator under test, in every case the cooling period must not be less than 2 hours [35]. At the end of the waiting period the insulator must be subjected to a HV conductor, and performance check is carried out while keeping the insulator at acceptable temperatures of 20°C - 70°C. Furthermore, after recovery the performance check must be repeated. Acceptable test results requirements are no damages must occur in the insulators under test, the insulator tolerance must not be exceeded.

Dry heat test is done according to IEC 62231, the temperature value for this test depends on the temperature range set by the operator and the nature of the insulator under test [35]. The insulator under test is places inside a chamber where the heat is raised to the specified temperature. Once the test is complete; the insulator under test can cool down to ambient temperature, and more performance tests are carried out [36]. Acceptable test results requirements are to ensure that the insulators do not exceed their operating limits or by those specified by the standards, and damages must not occur.

Salt mist test is required in cases where the insulator is exposed to moisture with different conductivities due to the salt level. The insulator must be tested in a way it's expected to be used. The test chamber must be kept closed and spraying of salt solution must continue without interruption during the entire conducting period [35]. The acceptable requirements tests are that there should be no major visible deterioration, and a performance check must be conducted. The Locomotive will be always on motion when is consume power from the OHTL, thus the movement will cause vibration, shock and bumps.

This means that the insulators will be subjected to the vibrations, shocks and bumps caused by the pantograph. Moreover, the Vibration, shock and bump test must be done using an equipment that will cause vibrations of sinusoidal form with adjustable amplitude and frequency. Alternatively, shock absorbing devices can be utilized in the insulator ends. According to EN 60068-2-27, insulators should not exceed vibration shocks of $50\ m/s^2$ longitudinal movement in a duration of $50\ ms$, $20\ m/s^2$ transverse movement in a duration of $20\ ms$ and a vertical movement of $10\ m/s^2$ in a duration of $20\ ms$ [37].

Chapter 4
Preliminary research results and analysis

The preliminary results and analysis are presented and discussed in this research study. The outcomes are to be compared to previously published results. The materials used for the outdoor insulators are simulated with similar properties to compile comprehensive results. This is done determine the effective ways for outdoor insulators to be utilized under harsh environmental conditions such as ultraviolet rays, contamination and over-voltages over a long period of time. The ceramic (porcelain and glass) and non-ceramic (polymeric) insulters are simulated and analyzed with there are properties. The simulation provides a clear understanding about the outdoor insulators.

4.1 Porcelain Insulators

The simulated porcelain disc insulator is initially connected on a 100 kV HVDC, the electrode is connected on the high voltage side and the metal cap on the low voltage side. The porcelain is placed between the electrode and the metal cap to provide proper insulation. The simulation results shown in figure 6, demonstrates the voltage distribution of a clean porcelain insulator and figure 8 demonstrates the electric field distribution of a clean porcelain insulator. The voltage is distributed uniformly from the surface of the electrode towards the surface of the porcelain plate [5]. The insulator physical properties are shown in appendix A table A1 and table A2.

The metal cap is earthed, voltage is not distributed around its surface. Furthermore, the voltage distribution decreases from the high voltage end to the low voltage end. Voltage distributed in the surface of the electrode depends on the size, shape and the applied voltage on the electrode [9]. In addition, the size of the insulator and shape of the electrode must be able to withstand the applied to avoid insulation failure. The density plot in figure 7 indicates the field intensity due to the applied voltage in the electrode and the metal cap, from a low to a high potential.

9.500e+006 : >1.000e+007
9.000e+006 : 9.500e+006
8.500e+006 : 9.000e+006
8.000e+006 : 8.500e+006
7.500e+006 : 8.000e+006
7.000e+006 : 7.500e+006
6.500e+006 : 7.000e+006
6.000e+006 : 6.500e+006
5.500e+006 : 6.000e+006
5.000e+006 : 5.500e+006
4.500e+006 : 5.000e+006
4.000e+006 : 4.500e+006
3.500e+006 : 4.000e+006
3.000e+006 : 3.500e+006
2.500e+006 : 3.000e+006
2.000e+006 : 2.500e+006
1.500e+006 : 2.000e+006
1.000e+006 : 1.500e+006
5.000e+005 : 1.000e+006
<0.000e+000 : 5.000e+005

Figure 6: Voltage distribution of a clean porcelain insulator
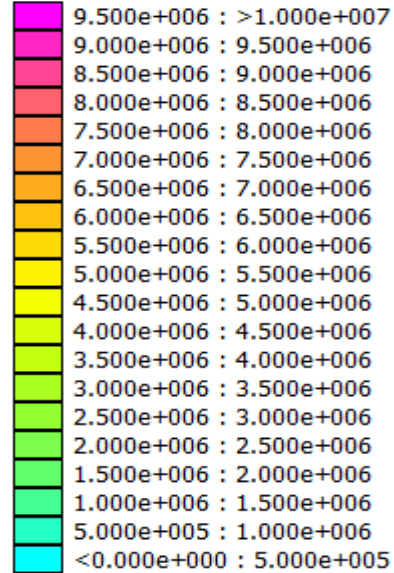
Figure 7: Density plot |V| Volts

The behavior of the porcelain insulator electric field distribution at initial voltage is shown in figure 8. Simulation results show that the electric field distribution radiates uniformly around the surface of the electrode, but the field line is not distributed linearly [19, 3]. The highest field density of the electric field lines with reduced width have more electric field lines radiating from the surface of the insulator [7, 38]. Fewer electric field lines appear in the low voltage side around the metal cap. The regions with high density radiate from the surface of the electrode connected in the HVDC line.

The electric fields can be reduced by increasing the size of the porcelain discs and reducing the applied voltage [39]. Electric field lines can create a path for flashover to occur [8]. The graph in figure 10 shows how the magnitude of electric field intensity decreases as it moves away from the surface of the electrode, on the high voltage side connected to the HVDC 100 kV transmission line. For a clean porcelain insulator, the maximum magnitude of the electric field is approximately 2.5×10^6 V/m. For electric fields greater than the magnitude of 3.0×10^6 V/m will result in leakage current and heat loss around the surface of the insulator [4, 21].
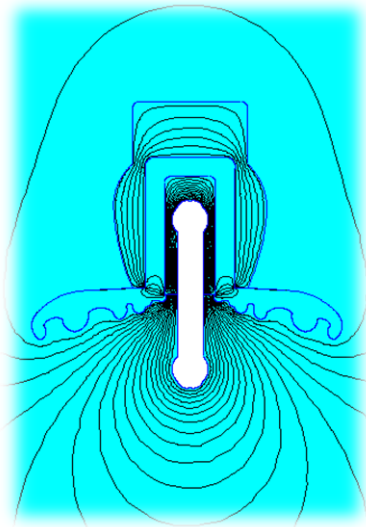
Figure 8: Electric field distribution of a clean porcelain insulator

2.447e+011 : >2.576e+011	
2.318e+011 : 2.447e+011	
2.190e+011 : 2.318e+011	
2.061e+011 : 2.190e+011	
1.932e+011 : 2.061e+011	
1.803e+011 : 1.932e+011	
1.674e+011 : 1.803e+011	
1.546e+011 : 1.674e+011	
1.417e+011 : 1.546e+011	
1.288e+011 : 1.417e+011	
1.159e+011 : 1.288e+011	
1.030e+011 : 1.159e+011	
9.016e+010 : 1.030e+011	
7.728e+010 : 9.016e+010	
6.440e+010 : 7.728e+010	
5.152e+010 : 6.440e+010	
3.864e+010 : 5.152e+010	
2.576e+010 : 3.864e+010	
1.288e+010 : 2.576e+010	
<2.980e-007 : 1.288e+010	
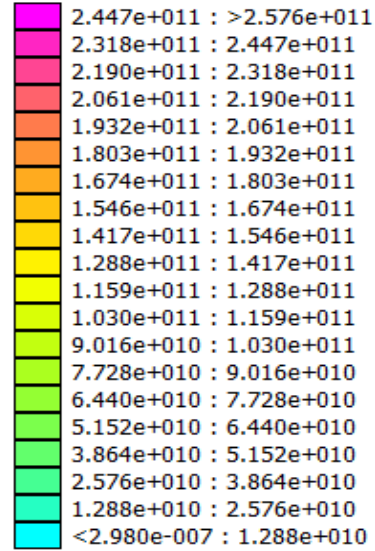
Figure 9: Density Field |E| V/m
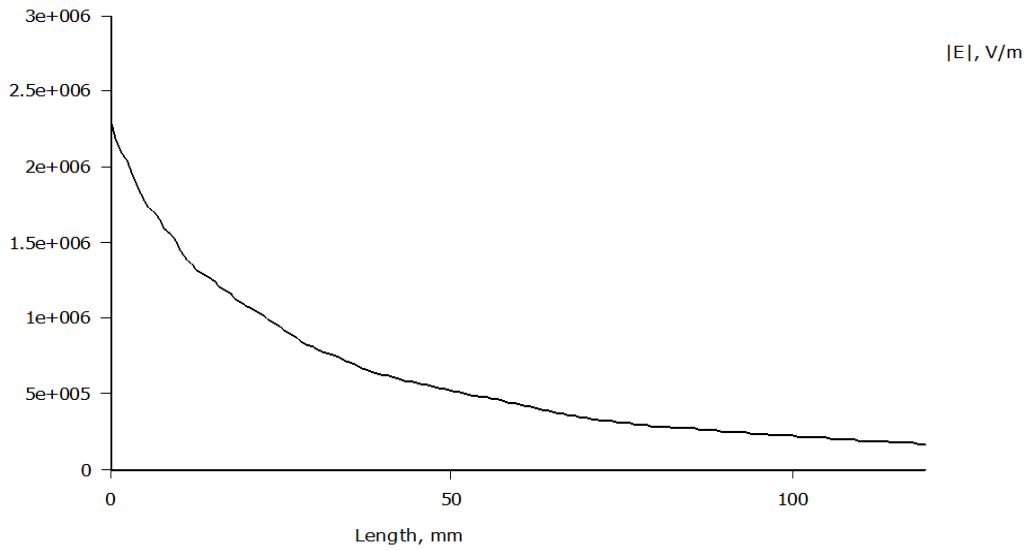
Figure 10: Magnitude of field intensity graph for a clean porcelain insulator

Porcelain insulators are prone to be polluted by dust and other dry contaminants that form an electrolytic layer around the surface of the insulator [26]. A thin layer of contaminants of approximately 1mm thick around the entire surface area of the insulator is used. The dry contaminants are slightly conductive with a conductivity of 0.0009 and a relative permittivity of 80F/m. The simulation results in figure 11 show the voltage distribution behavior of the porcelain insulator under contaminated conditions.

There is a non-linear and non-uniform voltage distribution, the contaminants have resistive properties that interrupts the charges around the surface of the insulator to cause disturbances for proper voltage distribution [19]. The resistivity of the contaminant layer creates a current path with voltage distributed around the surface of the insulator to form dry-band until flashover occurs [40, 41]. Furthermore, the contaminant layer can form an electrolytic layer that can cause a short circuit between the high and the low voltage ends to cause flashover [41].
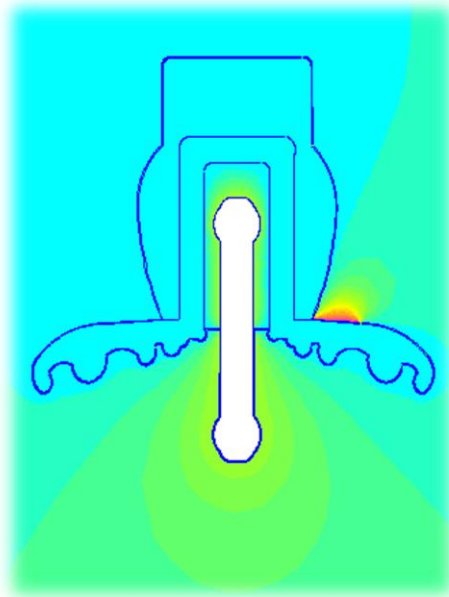
Figure 11: Voltage distribution of a contaminated porcelain insulator:

	2.591e+006 : >2.727e+006
	2.455e+006 : 2.591e+006
	2.318e+006 : 2.455e+006
	2.182e+006 : 2.318e+006
	2.046e+006 : 2.182e+006
	1.909e+006 : 2.046e+006
	1.773e+006 : 1.909e+006
	1.636e+006 : 1.773e+006
	1.500e+006 : 1.636e+006
	1.364e+006 : 1.500e+006
	1.227e+006 : 1.364e+006
	1.091e+006 : 1.227e+006
	9.546e+005 : 1.091e+006
	8.182e+005 : 9.546e+005
	6.819e+005 : 8.182e+005
	5.455e+005 : 6.819e+005
	4.091e+005 : 5.455e+005
	2.727e+005 : 4.091e+005
	1.364e+005 : 2.727e+005
	<0.000e+000 : 1.364e+005
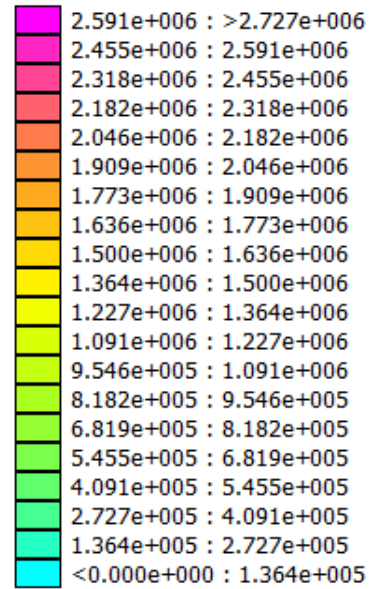
Figure 12: Density plot |V| Volts

The electric field distribution in figure 13 is interrupted by the dry contaminants. The contaminants interrupt the electric charge density in the insulator surface area [19]. The charges are trapped between the surface of the insulator and the contaminant layer [19, 13]. There are more electric field lines where the contaminant layer is thinner. The contaminants cause the insulator to heat due to leakage current [13]. When the porcelain insulator is heated it cracks or breaks since it brittle to cause flashover [3]. Comparing electric field simulation results obtained in figure 8 and figure 13.

The electric field distribution for a clean porcelain insulator in figure 8 has more visible field line radiating from the insulator but has a magnitude of the electric field of approximately 2.5×10^6 V/m. The electric field distribution in figure 13 has less visible field lines radiating from the insulator and has a magnitude of electric field that is approximately 3.2×10^7 V/m. The porcelain insulator exposed to contamination has a high magnitude of field intensity as shown in figure 15. In addition, a high magnitude of electric field intensity lead to flashover.
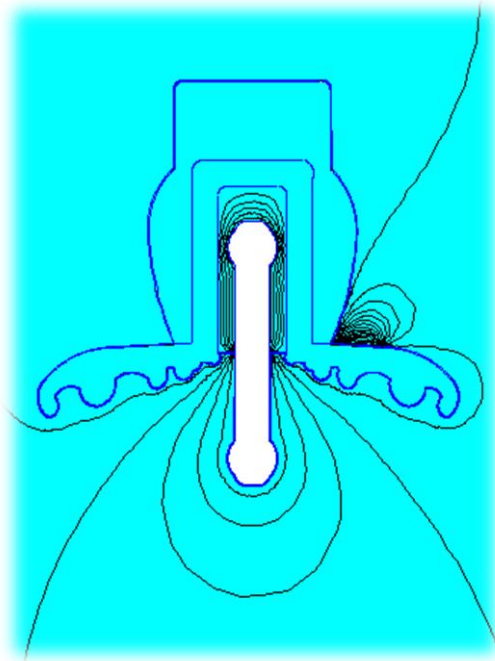
Figure 13: Electric field distribution of a contaminated porcelain insulator
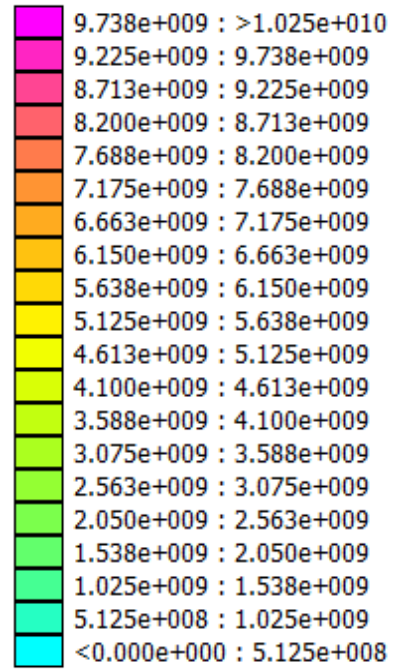
Figure 14: Density Field |E| V/m
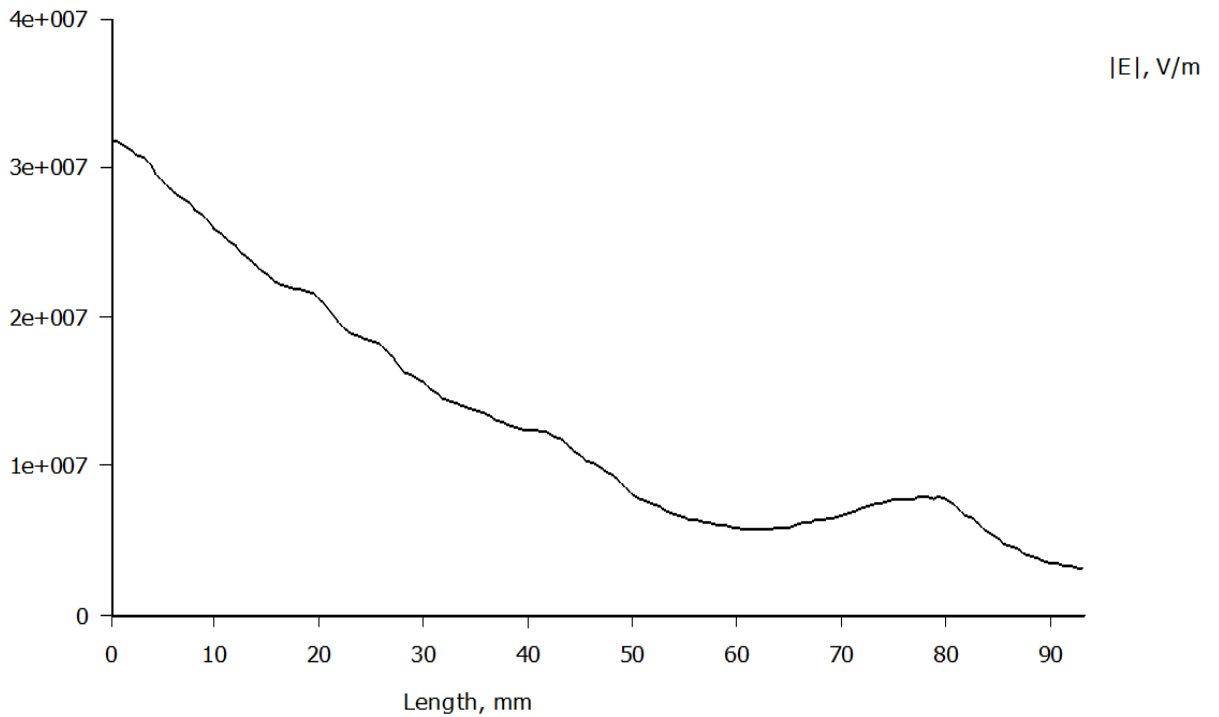
Figure 15: Magnitude of field intensity graph for a contaminated porcelain insulator

4.2 Glass Insulators

Glass insulators come in different sizes and shapes depending on the usage, a glass plate shaped insulator is used for 100kV HVDC simulation [10]. The glass insulator shares similar properties with the porcelain insulator except that the insulation part is composed of a fibre glass. Simulation results in figure 16 shows the voltage distribution, according to the simulation results there is a high-density field around the high voltage end of the electrode and a low-density field in the low voltage side. Figure 17 shows the voltage density field in the insulator.

The clean glass insulator shows proper insulation between the HVDC and the earthed metal cap, because the voltage distribution around the insulators shows complete isolation between the electrode and the metal cap. The surface of the insulator electrode under HVDC has a high voltage density distribution of approximately 9.5×10^4 V, however the surface of the insulator metal cap is earthed and has a low voltage density distribution of 0 V (zero volts) [10, 33]. These results depict that a clean glass insulator can provide proper isolation between the voltage ends that have a potential difference. The isolation proves better insulation for the clean glass insulator; therefore, flashover will not occur.
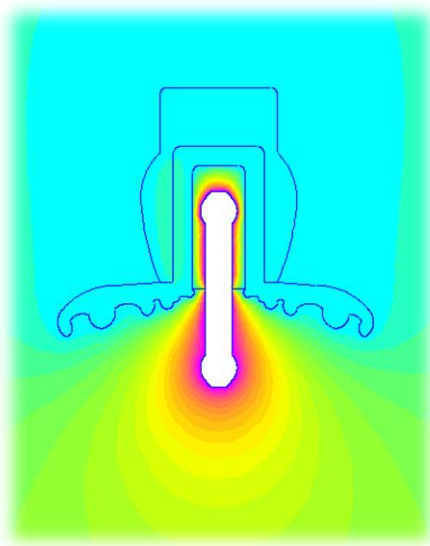
Figure 16: Voltage distribution of a clean glass insulator
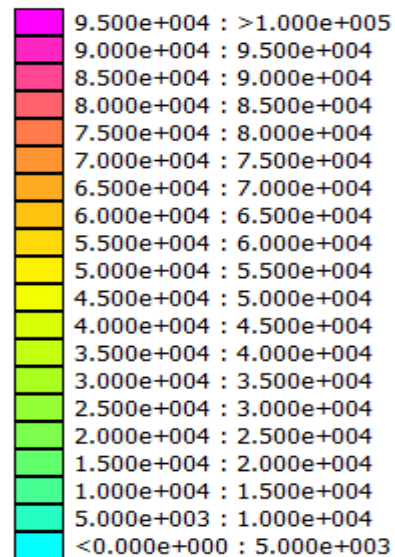
Figure 17: Density plot |V| Volts

The electric field behavior of the glass insulator is shown in figure 18. The electric field is distributed uniformly around the surface of the high voltage side and radiates away from the insulator. As a result, the electric field lines density decreases as the field line move from the surface of the electrode [23]. The relative permittivity (ε_r) of glass is 5F/m, which is lower than the relative permittivity of porcelain 5.9F/m, therefore glass has less electric field between the charges in comparison with porcelain operation under the same conditions.

Low density charged materials reduce the chances for electric fields to create a path for flashover to occur [4, 21]. The glass insulator has a low charge density, which helps reduce the chances of flashover under high density fields that are due to high voltages. For a clean glass insulator, the maximum magnitude of the electric field distributed in the insulator is approximately 3.5×10^6 V/m in figure 19. This implies that the glass insulator is prone to experience leakage currents and energy loss due to heat around the surface of the insulator, since it has a high-density electric field magnitude in comparison with porcelain insulators.

Simulation results in figure 18 show that there is a high-density electric field in the fibre glass between the electrode and the glass disc, thus a high-density charge which will result to energy loss due to heat losses [2, 4]. However, the insulator can be improved by installing a fiber glass that can withstand voltages greater than 100 kV HVDC. Figure 19 shows the electric field magnitude of the density field. The graph in figure 19 show the behavior of the field intensity magnitude across the clean glass insulator. The magnitude of electric field intensity decreases as the field lines radiate away from the surface of the electrode of the high voltage side connected to the HVDC 100 kV transmission line.
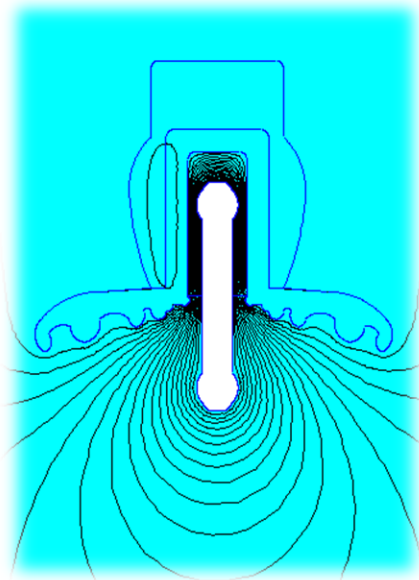
Figure 18: Electric field distribution of a clean glass insulator

■	9.499e+008 : >9.999e+008
■	8.999e+008 : 9.499e+008
■	8.499e+008 : 8.999e+008
■	7.999e+008 : 8.499e+008
■	7.499e+008 : 7.999e+008
■	6.999e+008 : 7.499e+008
■	6.499e+008 : 6.999e+008
■	5.999e+008 : 6.499e+008
■	5.499e+008 : 5.999e+008
■	4.999e+008 : 5.499e+008
■	4.499e+008 : 4.999e+008
■	3.999e+008 : 4.499e+008
■	3.500e+008 : 3.999e+008
■	3.000e+008 : 3.500e+008
■	2.500e+008 : 3.000e+008
■	2.000e+008 : 2.500e+008
■	1.500e+008 : 2.000e+008
■	9.999e+007 : 1.500e+008
■	4.999e+007 : 9.999e+007
■	<1.228e-009 : 4.999e+007
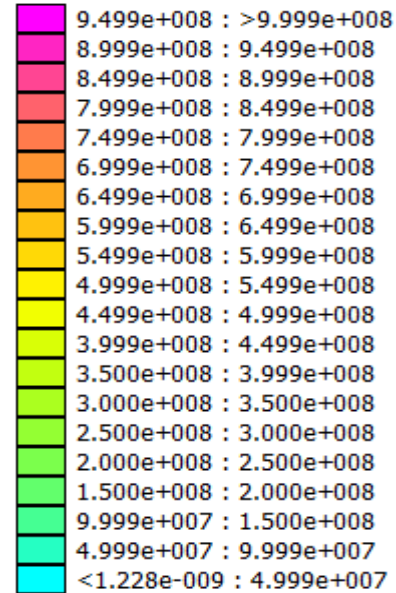
Figure 19: Density Field |E| V/m
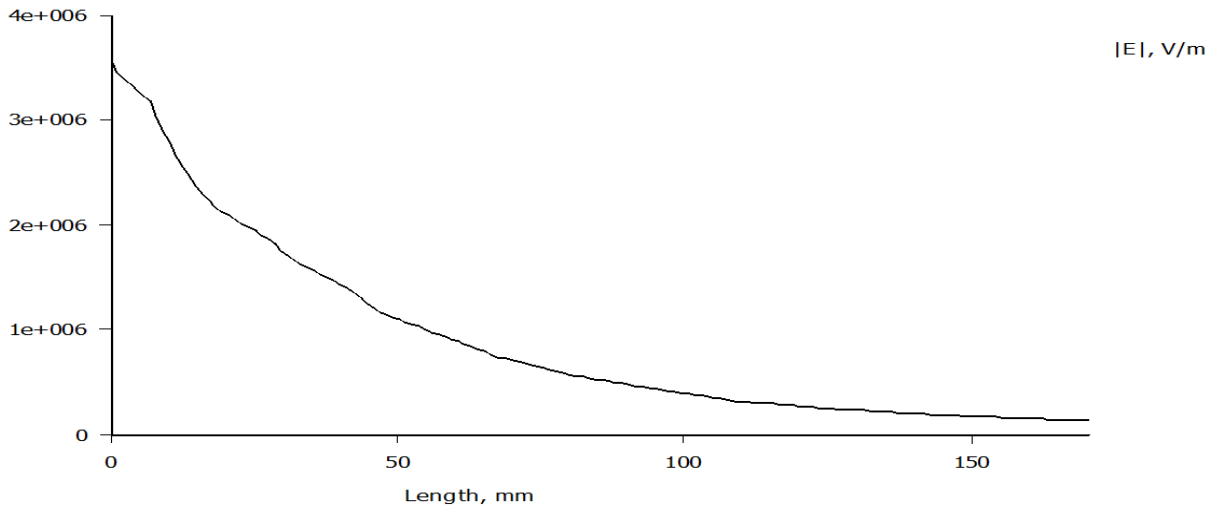
Figure 20: Magnitude of field intensity graph for a clean glass insulator

The simulation results of a contaminated glass insulator shown in figure 21, the insulator shows a non-linear voltage distrubution behavoir. The flashover voltage is higher in contantaminated conditions compared to a clean insulator [2]. A layer of dry contaminants with a thickness of approximately 1mm around the surface area of the glass insulator is used. The dry contaminants are slightly conductive with a conductivity of 0.0009 and a relative permittivity of 80F/m. The simulation results in figure 21 shows that the magnitude of voltage distribution behavior of the glass insulator under contaminated conditions is higher than that of a clean glass insulator.

In addition, glass insulators are prone to crack and break when operation under high electric field above the glass heating tolerance. The contaminants have resistive properties that may interrupt the charges around the surface of the insulator. The contaminants negatively affect the voltage distribution [19]. The resistivity of the contaminant layer creates a current path with voltage distributed along the surface of the insulator to form dry-bands where flashover is likely to occur [40, 41]. Furthermore, the contaminants in the surface of the insulator can form an electrolytic/conductive layer that creates a short circuit between the high and the low voltage ends that will result to a complete flash flashover [41].
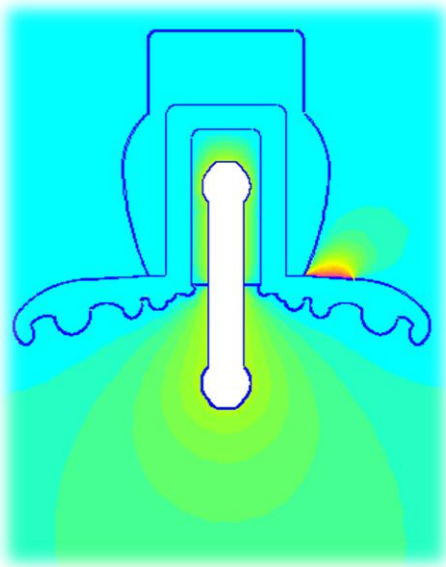
Figure 21: Voltage distribution of a contaminated glass insulator

	2.589e+006 : >2.726e+006
	2.453e+006 : 2.589e+006
	2.317e+006 : 2.453e+006
	2.180e+006 : 2.317e+006
	2.044e+006 : 2.180e+006
	1.908e+006 : 2.044e+006
	1.772e+006 : 1.908e+006
	1.635e+006 : 1.772e+006
	1.499e+006 : 1.635e+006
	1.363e+006 : 1.499e+006
	1.227e+006 : 1.363e+006
	1.090e+006 : 1.227e+006
	9.540e+005 : 1.090e+006
	8.177e+005 : 9.540e+005
	6.814e+005 : 8.177e+005
	5.451e+005 : 6.814e+005
	4.088e+005 : 5.451e+005
	2.726e+005 : 4.088e+005
	1.363e+005 : 2.726e+005
	<0.000e+000 : 1.363e+005
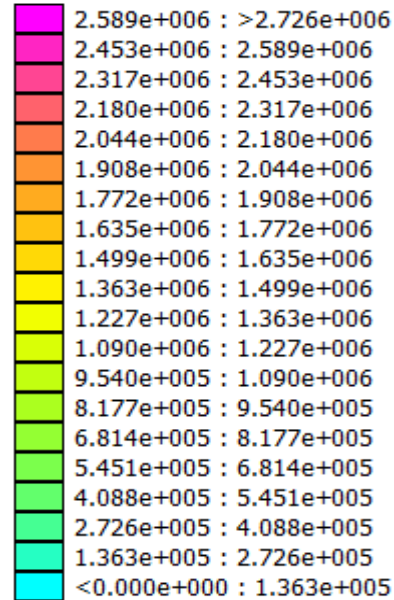
Figure 22: Density plot |V| Volts

The dry contaminants in the surface of the glass insulator interrupts the electric field distribution as shown in figure 23. The electric charge density around the surface area of the insulator is interrupted [19]. The charges that induce the electric fields are trapped between the surface of the insulator and the electrolytic layer caused by the contaminants [19, 13]. More electric field lines radiate where the contaminant layer thickness is less than 1mm. The electric field density has a high magnitude; therefore, it causes the insulator to heat due to leakage currents [13]. When the glass insulator is heated it cracks or breaks since it brittle, which leads to flashover [3]. The electric field distribution for a clean glass insulator in figure 19 has more visible field lines radiating from the surface of the high voltage side of the insulator but has a magnitude of the electric field of approximately 2.6×10^6 V/m.

The electric field distribution in figure 23 has less visible electric field lines radiating from the surface of the insulator and the magnitude of the electric field lines is approximately 2.5×10^8 V/m. Therefore, HVDC glass insulators exposed to contaminats have a high magnitude of electric field intensity in comparison with a clean glass insulator as shown in figure 25. In addition, a high magnitude of electric field intensity leads to flashover. The magnitude of electric field intensity of a contaminated glass insulator is higher than that of a contaminated porcelain insulator. The graph behavior for all simulated ceramic insulators is similar but have different magnitudes of electric field intensity.
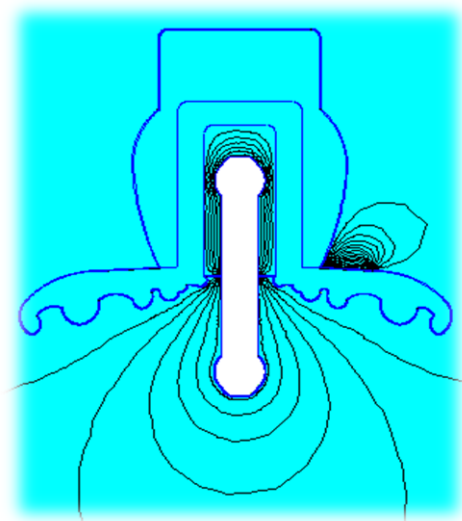
Figure 23: Electric field distribution of a clean glass insulator
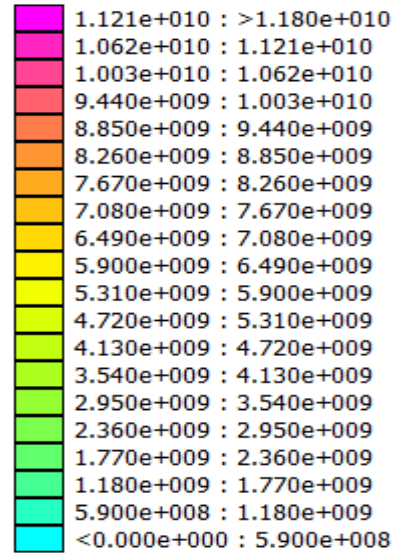
Figure 24: Density Field |E| V/m
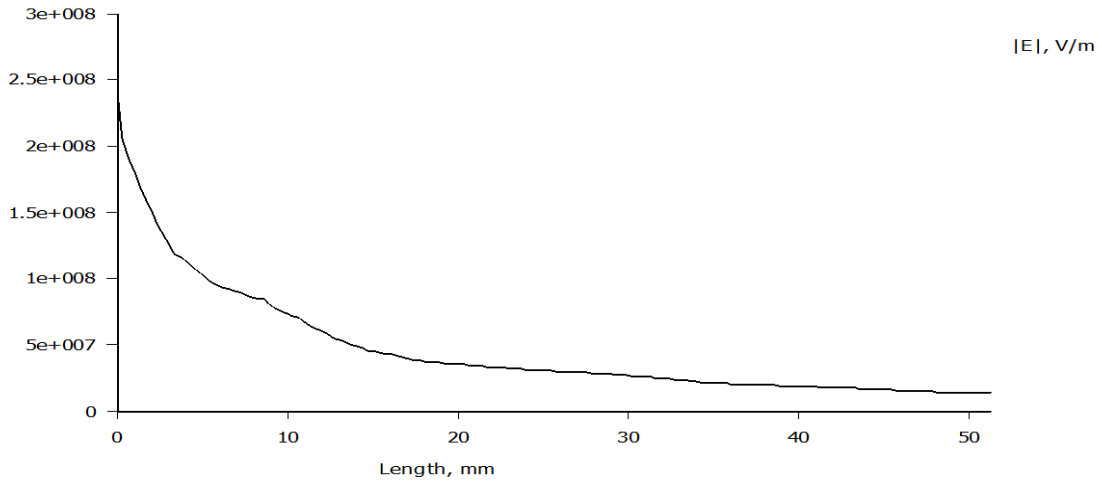
Figure 25: Magnitude of field intensity graph for a contaminated glass insulator

4.3 Polymeric Insulators

The simulated polymeric insulator in figure 26 shows the voltage distributed under 30 kV HVDC on the high voltage side and earthed at the low voltage side. The voltage applied is uniformly distributed and gradually decreases from the high voltage end to the low voltage end for a clean polymeric insulator. The strong mechanical fibre glass in the center of the insulator has voltage distributed between the minimum and maximum magnitude density voltage. There is a zero-voltage density magnitude at the low voltage side and a voltage density magnitude of approximately 2.8×10^4 V at the high voltage side.

The results signify that the insulator provides proper isolation between the low and high voltage ends, therefore flashover does not occur for a clean polymeric insulator. Simulation results of a clean polymeric insulator installed with a corona ring in figure 27 illustrates the voltage distribution. The radius of the corona ring used is 100 cm and 3 cm for the conductor. The corona ring experiences a fixed voltage of 1kV that is due to the charges on the electric field of the high voltage side. Furthermore, voltage distributed along the insulator with a corona ring has of density voltage with a low magnitude. The corona ring reduces voltage distribution to ensure better isolation between the low and high voltage ends.

In addition, polymeric insulators have a better electric performance with a corona ring installed and flashover is reduced. The corona ring prevents the voltage distributed from the high voltage side to reach the low voltage side, therefore preventing flashover. The strong mechanical fibre glass in the center of the insulator in figure 27 has a less density voltage magnitude of approximately 1.8×10^4 V distributed between the minimum and maximum magnitude density voltage. The voltage density magnitude is shown in figure 28. The voltage distributed from the high voltage side circulates around the surface of the corona ring, preventing it to move towards the low voltage side.
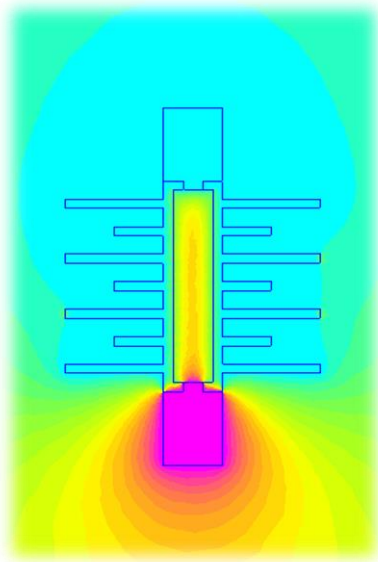
Figure 26: Voltage distribution of a clean polymeric insulator without a corona ring
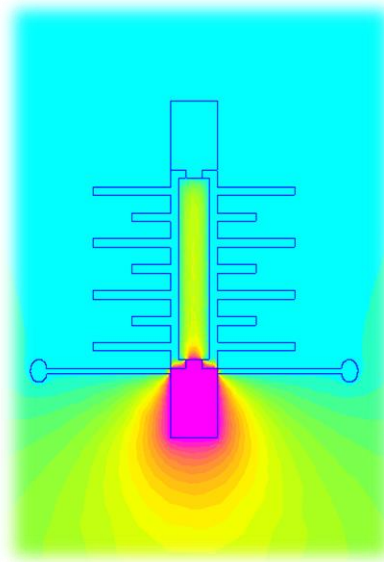
Figure 27: Voltage distribution of a clean polymeric insulator with a corona ring
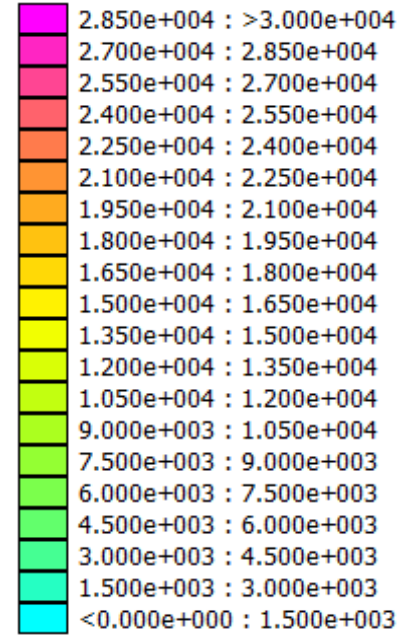
Figure 28: Density plot |V| Volts

Simulation results in figure 29 illustrates the behavior of the electric field lines as they move towards the links between the metallic and insulating material for the clean polymeric insulator without a corona ring. The electric field line creates a path that may lead to insulation failure and electric discharges that lead to energy losses [19]; therefore according to simulation results in figure 29, the clean polymeric insulator is prone to experience flashover if a corona ring is not installed. Furthermore, figure 30 also defines the vector plot line of the electric field direction. The vectors arise from the high voltage side into the low voltage side. The vector creates a type of circle across the insulator, another pair of field vector line are formed in the fiberglass inside of the insulator.

After the installation of the corona ring, the electric field is distributed uniformly across the insulator, while significantly reduces the chance of flashover by preventing the electric field line to radiate towards the low voltage side to provide proper isolation between the voltage ends. The corona reduces the electric field discharges, therefore reducing energy loss that is due to high electric field discharges in the high voltage side. The graphs in figure 32 and 33 show the behavior of the field intensity magnitude across the polymeric insulator with and without a corona ring. The magnitude of electric field intensity decreases as the field lines radiate away from the surface of the high voltage side connected to the HVDC 30 kV transmission line. The magnitude of the electric field intensity in figure 32 and 33 is approximately 4.1×10^4 V/m and 1.6×10^5 V/m, which agrees with the electric field behavior in figure 29 and 30.
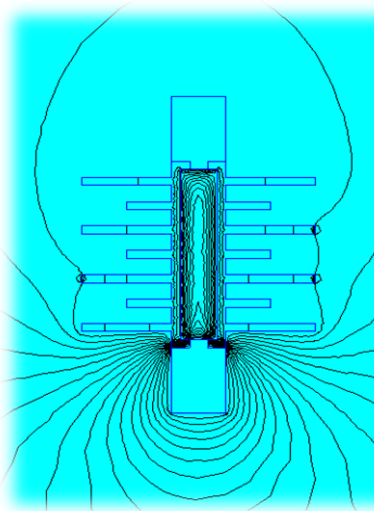
Figure 29: Electric field distribution of a clean polymeric insulator without a corona ring
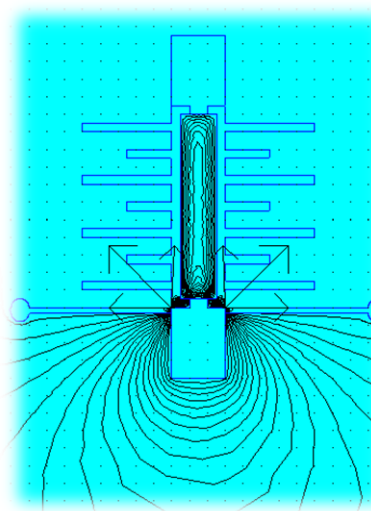
Figure 30:Electric field distribution of a clean polymeric insulator with a corona ring
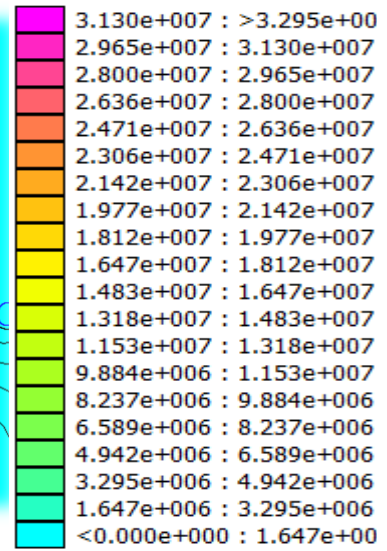
Figure 31: Density Field |E| V/m
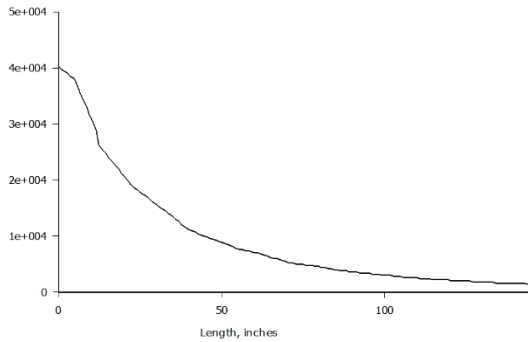

Figure 32: Magnitude of field intensity graph for a clean polymeric insulator without a corona ring
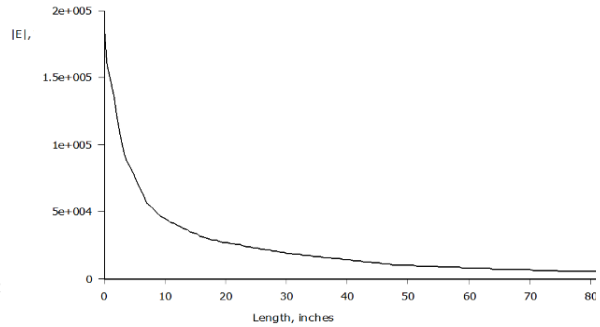
Figure 33: Magnitude of field intensity graph for a clean polymeric insulator with a corona ring

Interpreting simulation results in figure 34, which show a very interesting voltage distribution behavior on the high voltage end. A water drop with a relative permittivity (ε_r) of 88.4 F/m and a conductivity of 0.009 S/m is placed in the HVDC end at 30 kV. The water drop reduces the density magnitude of the voltage distribution, therefore interrupting the voltage distribution. Additionally; water is conductive, which might course a path to connect the insulator end to cause flashover. The insulator will not function properly if there will be high quantities of water trapped in the insulator surface.
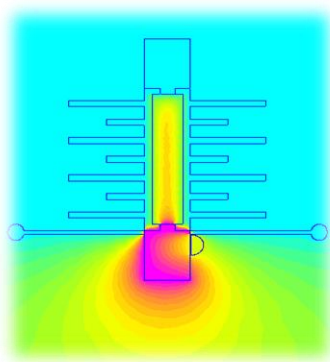
Figure 34: Voltage distribution of a wet insulator with corona ring
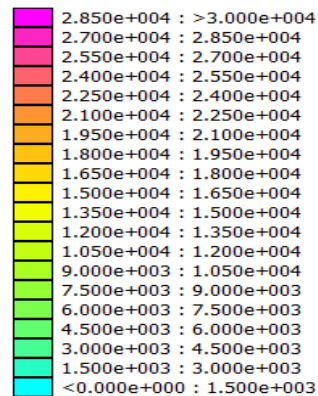
Figure 35: Density plot |V| Volts

Interpreting simulation results in figure 36 shows that the electric field distribution of the polymeric insulator when there is a drop of water in the surface of the insulator and the corona ring placed at the high voltage side. The maximum value of the electric field at the high voltage side of the insulator decreases, since the corona ring modifies the magnitude, shape and direction of the electric field intensity [10, 26]. These electrical fields might lead to the puncture of sheds in excess conditions [7].
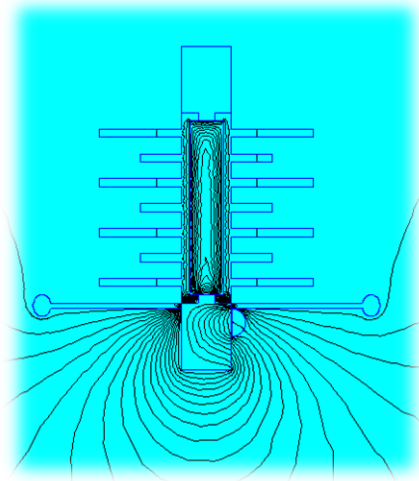
Figure 36 and Electric field distribution of a wet insulator with corona ring

| 3.143e+007 : >3.308e+007 |
| 2.977e+007 : 3.143e+007 |
| 2.812e+007 : 2.977e+007 |
| 2.646e+007 : 2.812e+007 |
| 2.481e+007 : 2.646e+007 |
| 2.316e+007 : 2.481e+007 |
| 2.150e+007 : 2.316e+007 |
| 1.985e+007 : 2.150e+007 |
| 1.819e+007 : 1.985e+007 |
| 1.654e+007 : 1.819e+007 |
| 1.489e+007 : 1.654e+007 |
| 1.323e+007 : 1.489e+007 |
| 1.158e+007 : 1.323e+007 |
| 9.924e+006 : 1.158e+007 |
| 8.270e+006 : 9.924e+006 |
| 6.616e+006 : 8.270e+006 |
| 4.962e+006 : 6.616e+006 |
| 3.308e+006 : 4.962e+006 |
| 1.654e+006 : 3.308e+006 |
| <0.000e+000 : 1.654e+006 |
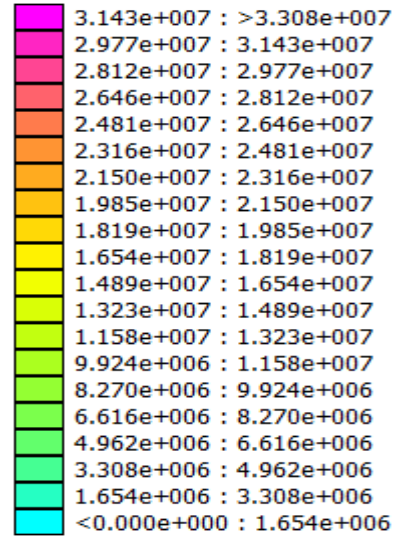
Figure 37: Density Field |E| V/m

The corona ring is primarily installed to control the electric field distribution on the voltage ends of the polymeric insulator under high voltage distribution and reduce corona to minimize insulation failure, which leads to flashover [21]. Thus, considering a wet polymeric insulator with a corona ring. Figure 36 illustrates the electric field distribution across the insulator if a single water drop is placed on the surface of the insulator. The spikes in figure 38 signify the enhancement of the electric field intensity [22]. The magnitude of the electric field intensity of the spike due to the water drop in figure 38 is approximately 1.8×10^5 V/m, and the average magnitude of the electric field intensity across the insulator is approximately 5.5×10^4 V/m.
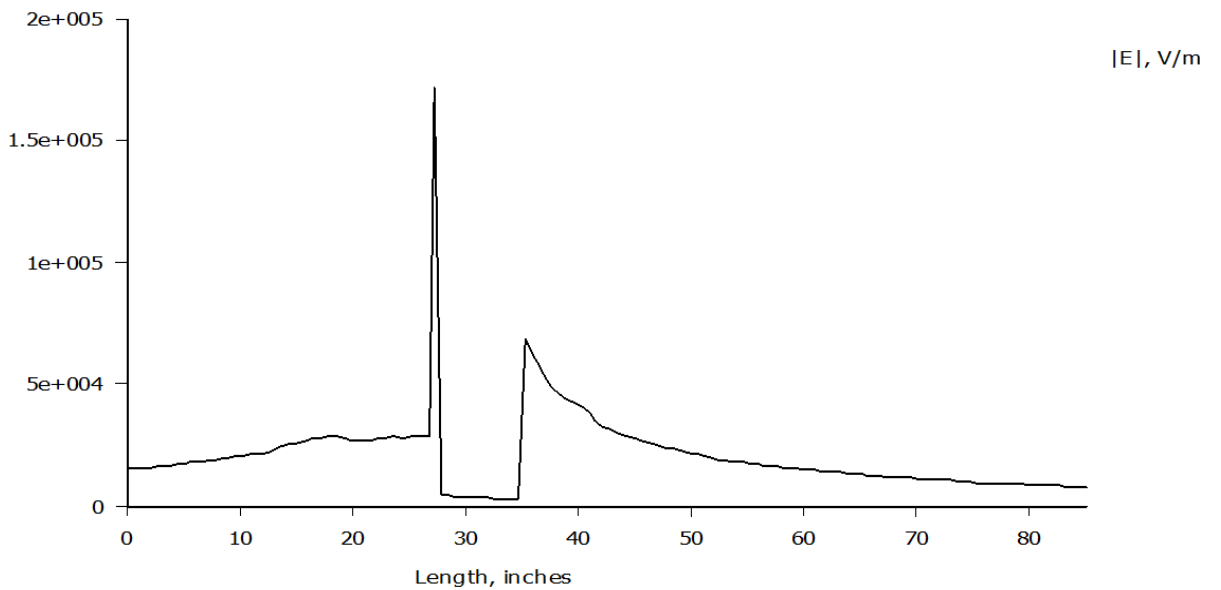

Figure 38: Magnitude of field intensity graph for a wet polymeric insulator with a corona ring

Chapter 5
Main research results and analysis

This chapter covers the main research results and analysis backed up by other theories from previously done studies. The numeric results are recorded through MATLAB simulation for different voltage levels and tabulated in appendix B. The results are presented graphically from the numerical values obtained through simulations. The simulated test circuits are presented in chapter 3. The conductivity and leakage current for different high voltage values is analyzed using graphical results from the figures presented in this chapter.

The main events that lead to flashover of contaminated insulators operating under high AC and DC voltages includes: the development of a conductive layer, the leakage current that leads to the formation of dry bands and of partial arcs that occur in the surface of the insulator [42]. Insulation for a contaminated HVDC system is more complex due to the extended duration of partial arcs and the electrostatic forces that create a path for flashover due to the negative and positive charges [43]. The insulator dimensions are chosen accordingly to maintain a safe creepage distance for the insulator operating under different contamination levels [44, 43].

Considering a wet-contaminant test method, the insulator is wetted by water drops while increasing the voltage until flashover occurs [45]. The salt fog test is done when the leakage resistance has decreased to its minimum value after the insulator has been contaminated, wetted and dried. The equivalent salt deposition density (ESDD) method is done through simulation of an insulator subjected to a HVDC and HVAC with a water solution with different electrical conductivities [46, 45]. The leakage current is obtained by placing the wet contaminated insulator in an electrical circuit to measure its leakage resistance by applying a measured voltage level [45].

5.1 Effect of conductivity

Figure 39 shows that as the conductivity of the contaminants increases, the flashover voltage decreases non-linearly. Furthermore; when the conductivity of the contaminant layer increases to a magnitude that is greater than approximately 4 μs for the simulated insulator models, the flashover voltage becomes slightly affected as the flashover voltage does not change for all simulated insulator models [47, 26]. This is because greater conductivities tend to increase the propagation speed of the streamers which leads to flashover for low voltage magnitudes [48].
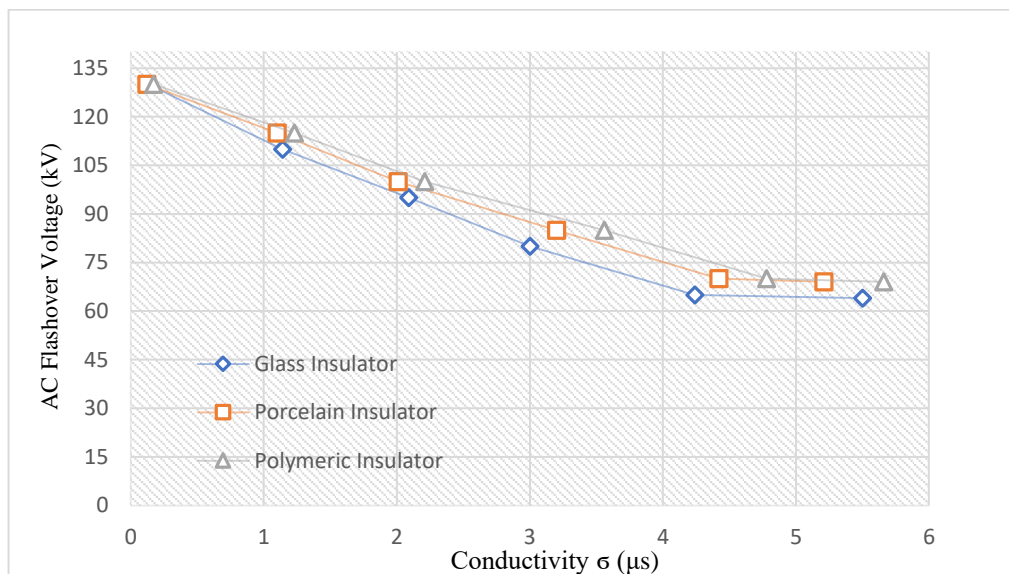

Figure 39: Flashover due to the conductivity layer in the insulator surface

Additionally, the graphical results in figure 39 show that the dielectric properties of the insulators become weaker when the conductivity of the contaminants is relatively high. This is because the contaminants become conductive to allow current to pass between the low and high voltage ends, which causes flashover to occur at lower voltages. The flashover voltage of the glass insulator is slightly less than that of the porcelain and polymeric insulators: this is because the fiberglass material has weaker dielectric properties [47], which makes the glass insulator most unsuitable performing under contaminants with conductivity higher than 0.10 μs.

However, the polymeric insulator performs better than the glass and polymeric insulators as the conductivity of the contaminant layer increases; this is because the silicon rubber material has better dielectric properties to prevent flashover at high voltage [44]. The relationship between the conductivity of the contaminants and the AC flashover voltage of the three insulators tested has a similar downtrend behavior but flashover occurs in different conductivity values. The results confirm that the dielectric rigidity of uniformly contaminated insulators is weaker than that of non-uniformly contaminated insulators.

The uniformly distributed contaminants have the same conductivity throughout the surface of the insulator, which creates a complete current path for flashover to occur. However; the non-uniform distributed contaminants have different conductivities and gaps in the surface of the insulators, which makes it difficult for the current to find a complete current path for flashover to occur. Therefore, flashover voltage depends completely on the uniformity and the conductivity of the contaminants in the surface of the insulator. According to previously done studies, the flashover voltage decreases as ESDD increases [47].

However, the ESDD is directly proportional to leakage current. Therefore, it is evident that as the leakage current increases, the voltage at which flashover voltage occurs decreases, which corresponds with results obtained in figure 39. This means that the leakage current is inversely proportional to the flashover voltage. Furthermore; this means that for relatively high conductivity of contaminants and salt deposit density, the insulators are more prone to be subjected to flashover during normal operating voltages. The contaminants in the surface of the insulator create resistance (surface resistance) which is inversely proportional to the ESDD [46]. Theoretically; this means that as the surface resistance increases, the ESDD and leakage current decreases.

5.2 Leakage current for a clean insulator

Leakage current is monitored through MATLAB simulation to understand and analyses data performance when the insulator is clean or subjected from different types of outdoor contaminants. The insulator dimensions and properties are applied mentioned in chapter 3 are applied to the insulator model undertest. This is done to achieve feasible and comprehensive results through simulation tests. Leakage current test for a clean glass, porcelain and polymeric insulator was done and shown in figure 40. This shows the insulator performance in relation to the leakage current operating in different AC voltage levels.

The insulators are electrically modelled as a series of capacitors (C) and resistors (R) connected in parallel; where C represents the dielectric capacity and R represents the surface leakage resistance [23]. The capacitance is measured between the high voltage side and ground. The dielectric capacity of porcelain, glass and polymeric insulators is approximately 30 pF, 25pF and 10 pF and the leakage current are obtained by multiplying the HVAC and capacitance product by 377. Therefore, using the formula I=377V_ac C will give the anticipated leakage current under the operating overhead transmission line [20]. The leakage current calculations are done and tabulated in table B1 of appendix B. The calculated results are presented graphically in figure 40.
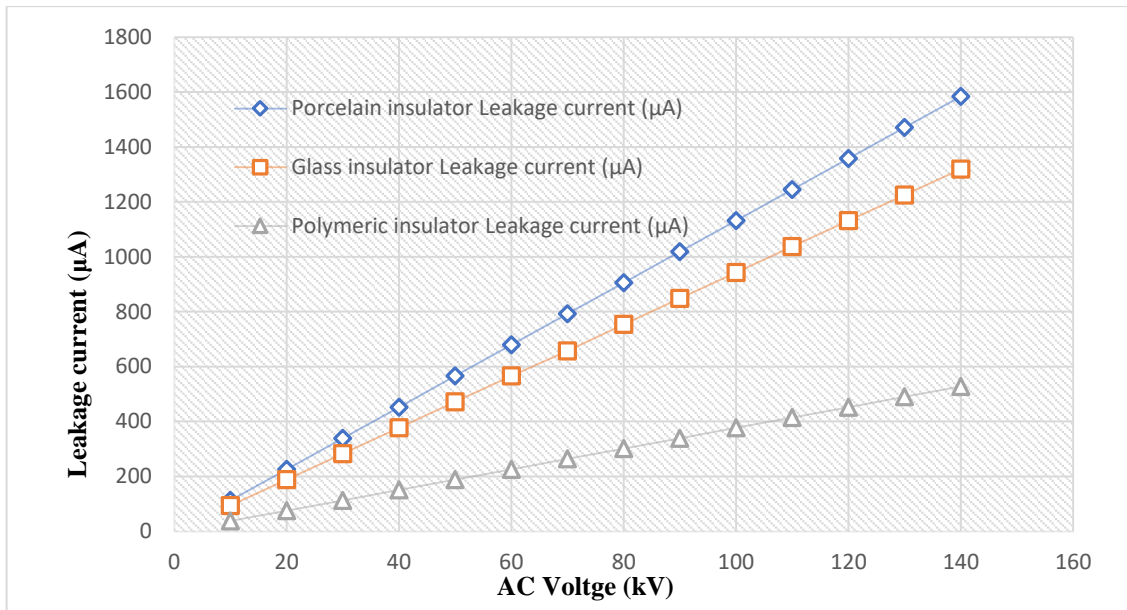
Figure 40: Leakage Currents for a clean Porcelain, Glass and Polymeric insulators under HVAC

Furthermore, figure 40 depicts the relationship between the leakage current and the AC voltage. The leakage current increases linearly as the voltage increases. The polymeric insulator has less leakage current compared to the glass and porcelain insulators; thus, the polymeric insulator is less prone to flashover [32]. However, the glass and porcelain insulators have high magnitude leakage current due to the dielectric capacity. Additionally, this means that the porcelain and glass insulators are much prone to flashover in comparison to the polymeric insulator [49].

The calculated leakage current is completely dependent on the dielectric capacity and the applied AC voltage. The dielectric capacity of a polymeric capacity is less than that of a glass and porcelain insulator. Therefore, the polymeric insulator will experience less leakage current.

5.3 Leakage current for a contaminated insulator

The leakage current creates a path to flow through the contamination layer which changes the conductivity of the insulators [30]. The contaminated layer heats up due to the leakage current path which eventually results in the loss of electrical energy as heat dissipation [26]. The leakage current measurement is directly affected by the different conductivities used for different contamination levels and the type of contaminants used. Furthermore, the leakage current shows a similar behavior if the contaminant layer is dry, but the currents leak in greater magnitudes if the contaminant layer is wet.

For dry contaminants in the surface of the insulators, a linear behavior of the leakage current as a function of AC voltage is shown in figure 40. However, for a wet contaminant layer in the surface of the insulator, and exponential behavior of the leakage current as a function of AC voltage is shown in figure 40. The leakage currents are measured and recorded through a MATLAB digital multimeter tool for different voltage levels [50, 30]. The leakage currents may change depending on the resistive properties of the conductive layer, which may be affected by the water temperature, the salt level for the conductivity of water and the relative permittivity of the dry contaminants.
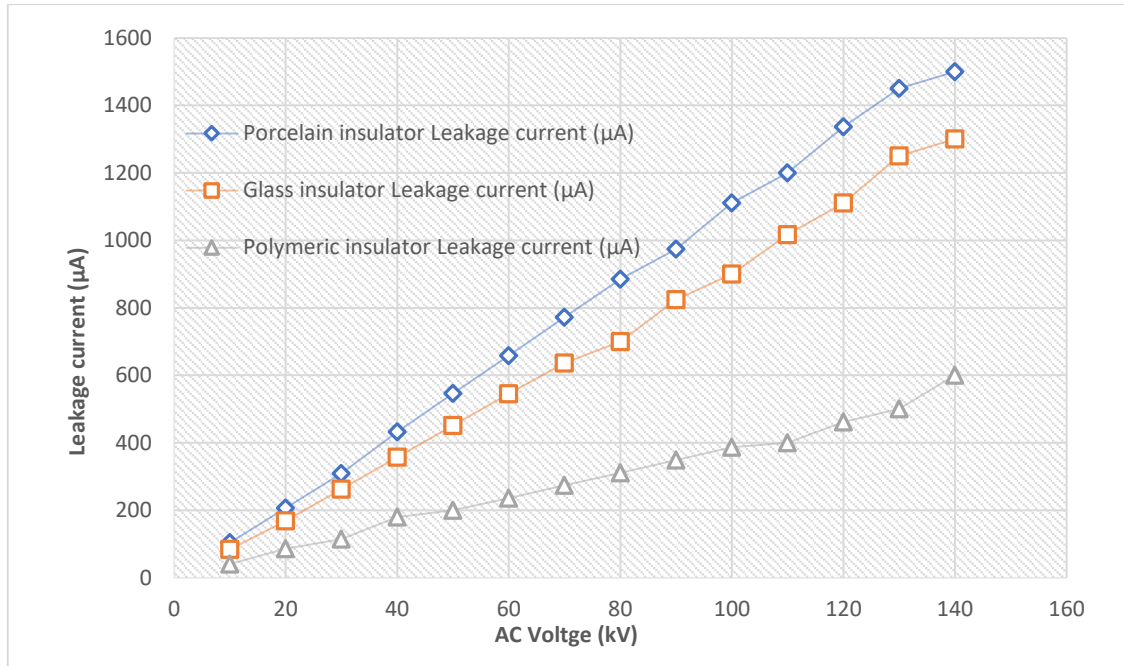
Figure 41: Leakage currents for dry contaminated Porcelain, Glass and Polymeric insulators under HVAC
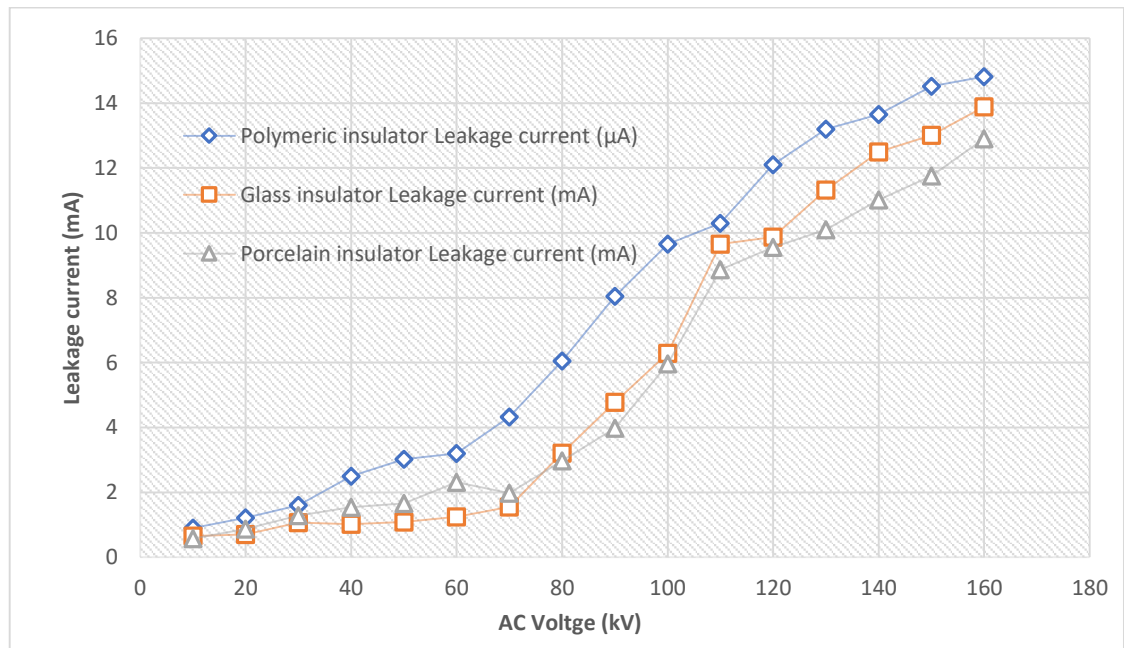
Figure 42: Leakage Currents for wet contaminated Porcelain, Glass and Polymeric insulators under HVAC

According to the graphical results in figure 42, the wet contaminated polymeric insulator experiences a high magnitude of leakage current. Therefore, the polymeric insulator does not perform well under wet conditions of a HVAC system. On the other hand, the glass insulator performs well until it reaches approximately 80 kV and the porcelain insulator eventually performs better from approximately 80 kV, because it has less leakage current operating under wet conditions. This means that the porcelain insulator has better hydrophilic properties. However, the polymeric is composed of a silicon rubber which has hydrophobic properties to prevent moisture to rest in the surface of its shreds.
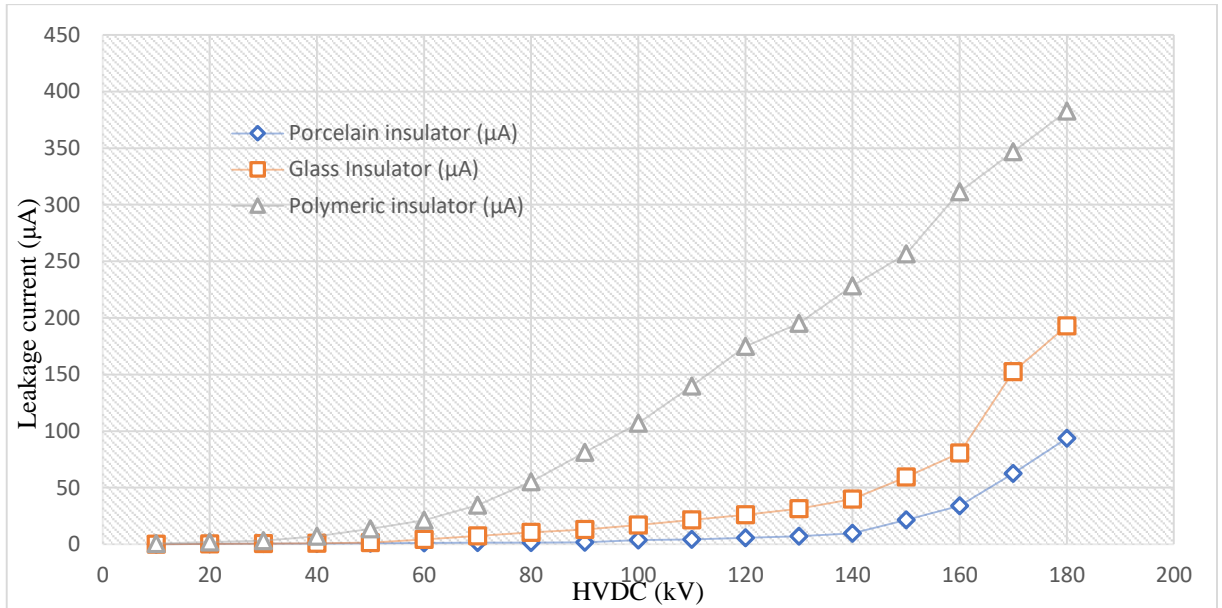
Figure 43: Leakage Currents for dry contaminated Porcelain, Glass and Polymeric insulators under HVDC
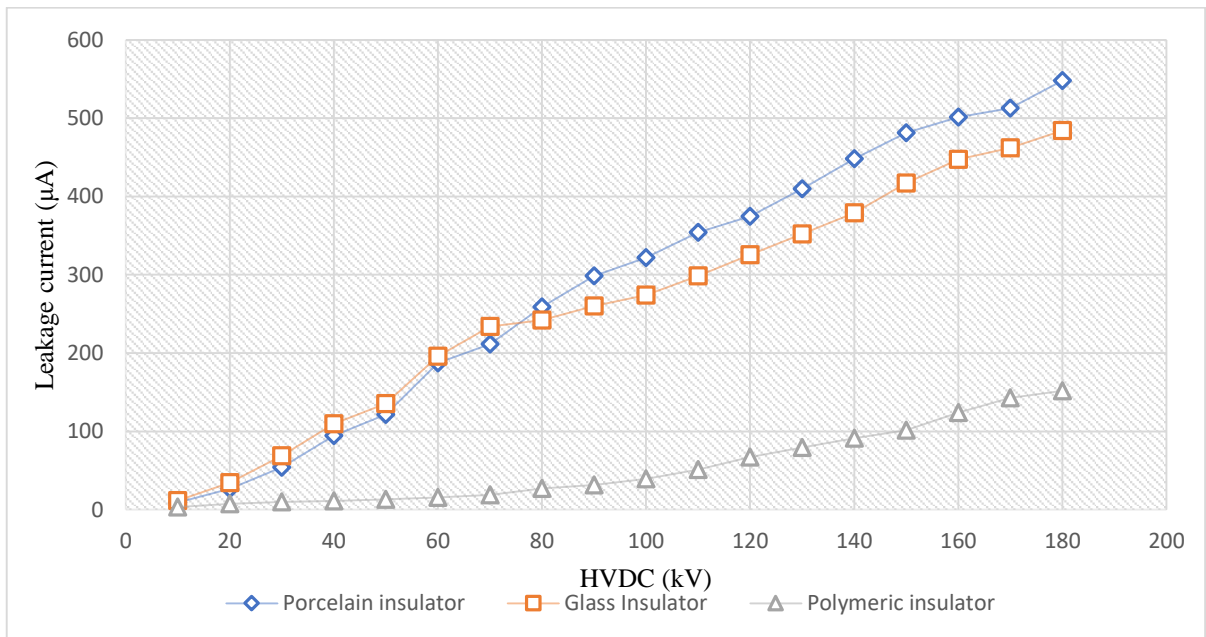
Figure 44: Leakage Currents for wet Porcelain, Glass and Polymeric insulators under HVDC

According to the graphical results shown in figure 41, the leakage current is measured through a MATLAB simulation model. The device under test is set to similar properties of each insulator type with dry contaminants under different HVDC levels. The insulator performances differ from different HVDC levels [43]. The leakage currents increase exponentially with increasing voltage in figure 41. However, the polymeric insulator performs poor; since it allows more leakage current than the glass and polymeric insulator, which eventually increases the chances of flashover to occur [51]. Therefore, the polymeric insulator is not suitable to perform under a dry contaminated area operating in HVDC [52].

The glass and porcelain insulators have a similar leakage current magnitudes and performance for HVDC from 0 to 45 kV until the glass insulator starts experiencing more leakage current. This is due to the resistive properties of glass with less resistance than the porcelain insulator, which allows a better path for leakage current for voltages greater than 45 kV [48]. It can be noted from figure 41 that the porcelain insulator performs better operation under all test HVDC levels. Therefore, a porcelain insulator is very preferable for HVDC system and OHT to be utilized in dry contaminated environments [44].

The leakage current magnitude might differ by changing the contamination layer thickness in the surface of the insulator. Moreover, referring to the graphical results in figure 44, the leakage current behavior for the porcelain and glass insulators is similar but different leakage currents magnitudes. The magnitude of the glass leakage current is greater than that of a porcelain insulator for HVDC from 0 kV to approximately 70 kV.

The porcelain insulator starts experiencing greater magnitudes of leakage currents for different HVDC levels from approximately 70 kV until flashover occurs [53]. This means that for any HVDC magnitude less than approximately 70 kV, the glass insulator will experience flashover under wet contaminated environments [54]. Furthermore, for a HVDC magnitude of more than approximately 70 kV, the porcelain insulator will experience flashover under wet contaminated environments [31]. Considering wet contaminated insulators in figure 44, the performance of the glass and porcelain insulators is affected by the water temperature.

However, the glass insulator can overcome thermal changes due to the fiber glass that does not absorb heat under high DC voltages, this prevents the moisture from heating-up in the surface of the insulator. Thus, the resistive properties of water do not change due to water temperature. Furthermore, the porcelain is composed of ceramic which heats-up under high DC voltages, this allows the moisture in the surface of the insulator coating to heat-up forming dry-bands to create current path [55]. The current path causes the insulator to experience flashover [52]. Considering the polymeric insulator operating in HVDC under wet contaminated condition in figure 44.

The graphical results confirm that the polymeric insulator performs better under wet contaminated conditions [49]. This is because the insulator is composed with silicone rubber which has hydrophobic properties to resist moisture in the surface of the insulator. Therefore; according to the simulation results, the porcelain insulator experiences less magnitudes of leakage current operating under wet contaminated conditions, which makes it the better insulator to be utilized in wet environmental conditions [46]. Therefore, flashover is less likely to occur. Considering a case when a small band arching starts, the leakage current becomes resistive in nature [31].

The simulation results might differ with the materials used for each insulator together with the dimensions and the shapes. The properties of each material can slightly change depending on if the insulator meets the IEC and SANS standards [35]. Furthermore, in a case of dry contaminants the insulator can be covered with dust, chemicals or other substances with different conductivities and moisture with different ESDD [45]. The mentioned factors might change over time and might affect the insulator performance over time.

However, the simulation results help to choose suitable insulators for a certain environment and voltage level for better and continuously improving insulation on the OHT systems of locomotives. The insulator dimensions are simulated according to standards on FEMM. Considering the relationship between the leakage current and dielectric strength is inversely proportional. If the dielectric strength of the insulator is high, therefore the resistance of the insulation is high. This results in less leakage current through the insulator.

This agrees with the graphical results shown in figure 44, meaning that that the polymeric insulator has a high dielectric strength in comparison with the porcelain and glass insulator.

Chapter 6
Conclusion and recommendation for future work

6.1 Conclusion

According to the results, the contaminants affecting the insulator performance differ depending on their conductivities. Contaminants with a lower conductivity have less effect on the insulator performance in comparison with contaminants with higher conductivity. The insulator is more prone to flashover when it is operating to its maximum rated voltages.

1. The insulator cannot perform to its maximum rating when it is contaminated, therefore the contaminants lower the insulator threshold voltage
2. The corona ring aids the distribution of electric fields around the corona ring on a clean or dry contaminated insulator however, a wet contaminated insulator performance with and without a corona ring is similar.
3. The graphical and qualitative results of a wet contaminated insulator show a similar performance trend. Therefore, installed corona rings on the insulator ends are not able to protect the insulator against flashover during wet conditions and some other methods should be introduced to protect the system against a high density of electric field to minimized or prevent the chances of flashover.
4. The experimental results show that the insulators can operate at higher AC supply voltages than on DC supply voltages. This is because there is a high current flow on DC supply in comparison to the AC supply on the same voltage level.
5. The voltage distribution is more uniformly distributed on an AC supply system and less electric field density. Thus, partial discharges are less on AC and the chances of flashover are minimal.
6. The leakage current increases with the present charges on the surface of the insulator for both AC and DC supply systems. However, there is a rapid increase in leakage current under a DC supply system

In conclusion, the increase of leakage current on the surface of the insulator is due to the increase of conductivity, which also alters the electric field distribution. The flashover is also dependent on the breakdown of air, which is influenced by the creepage distance and surface charges of the insulator. Therefore: the electric field, and creepage distance and breakdown voltage must be considered when specifying an insulator design for HVDC and HVAC system.

6.2 Recommendation for future work

The qualitative and quantitative properties of the insulator must be considered when improving insulator performance. Qualitative properties: such as the shape, size, and orientation of the insulator to be designed in such a way that it accumulates less or no contaminants on its surface. Quantitative properties: such as the resistivity and permittivity of the material used, the behavior and calculation of the leakage current, electric fields and voltage distribution for different applied voltage levels from an AC and DC generated source. Eventually, the continuation of this research study would assist in the development of improved standards for the exiting insulator to achieve better performance of insulators.

References

[1] H. M. S. B. a. M. M. Mirza Batalović, "Influence of Environmental Stresses on High Voltage Polymer Rod Type Insulator Performances," in *Electrical Engineering Department of Power Engineering*, Hrvatska.

[2] J. H. Y. L. L. S. S. X. Xingliang Jiangl, "Pollution Flashover Performance of Short Sample for 750kV Composite Insulators," *The Key Laboratory of High Voltage and Electrical New Technology of Ministry of Education,* vol. i, no. 1, pp. 1-4, 2004.

[3] H. F. Y. Z. q.-g. a. G. b. Chen Yong, "Study on Withstand Voltage Characteristics and Surface Electrical Field Distribution along Polluted Insulators," in *Wuhan High Voltage Research Institute of SGCC,Wuhan*, Xi'An Jiaotong University, Xi'an 710049, China, 2008.

[4] B. N. P. N. K. a. S. V.Muralidhara, "Study of Thermal-runaway tests on Insulators subjected to DC voltages," in *High Voltage Division*, Bangalore. India, 2008.

[5] J. Z. B. L. R. H. a. Z. S. Xinzhe YU, "Influence of cap-and-pin disc insulator profile on contamination flashover voltage," in *China Electric Power Research Institute*, Beijing, China.

[6] Z. Z. K. Z. W. L. a. Y. Xiaohuan Liu, "Analysis of the Pollution Accumulation and Pollution Flashover Performance of Outdoor 500kV Insulator String," *High Voltage Engineering and Application,* vol. III, no. 3, pp. 1-4, 2012.

[7] H. H. a. S. F. M.El-A. Slama, "Study on Influence of the No-Uniformity of Pollution at the Surface of HVAC Lines Insulators on Flashover Probability," *Electrical Engineering and High Voltage Laboratory of Oran, Faculty of Electrical Engineering,* pp. 1-5, 2007.

[8] P. W. E. G. H. B. Hassan Saadati, "Flashover Performance of Polluted Composite Insulators Under AC and Hybrid AC/DC Field Stress," in *Electrical Insulation Conference*, Hannover, Germany, 2016.

[9] S. a. D. M.RAVINDRAN, "Analysis and Modeling of Thermal Plant Pollution Performance in High Tension Ceramic Post Insulator with Epoxy Resin Coatings," in *3rd International Conference on Advances in Electrical, Electronics, Information, Communication and Bio-Informatics*, Tamilnadu, India.

[10] S. W. L. W. a. Z. G. Chuyan Zhang, "Pollution Flashover Performance of 220kV Glass Insulator Strings Covered with Incomplete Spraying PRTV Coatings," *Outdoor Insulator Performance ,* vol. I, no. 4, pp. 1-3.

[11] A S Krzma, M Albano and A Haddad, "Comparative Performance of 11kV Silicone Rubber Insulators using Artificial Pollution Tests," in *Advanced High Voltage Engineering*, Cardiff University, U.K..

[12] M. A. a. A. H. Adnan S Krzma, "Flashover Influence of Fog rate on the Characteristics of Polluted Silicone-Rubber Insulators," in *Advanced High Voltage Engineering*, Cardiff University, U.K..

[13] O. E. G. a. G. M. Amer, "Factors Affecting the Leakage current Bursts of High Voltage Polluted Insulators," Ciaro.

[14] J. C. D. L. K. X. M. Y. Y. C. R. L. a. F. Z. Youping Tu, "Study on the Aging Characteristics of Insulators Sheds," in *IEEE International Conference on Solid Dielectrics*, Bologna, Italy, 2013.

[15] S. 6.-2. a. I. 60815-2:2008, SOUTH AFRICAN NATIONAL STANDARD, Lategan Road Groenkloof: Published by SABS Standards Division, 2008.

[16] H. Yang, J. Zhou, Y. Li, L. Pang, X. Yang, Q. Zhang and X. Yu, "Effect of profiles on ac contamination flashover performance of large-tonnage suspension disc insulators," *IEEE Transactions on Dielectrics and Electrical Insulation,* vol. 21, no. 6, pp. 2476 - 2485, 2014.

[17] M. A. S. a. H. Ahmad, "Derivation of creepage distance in terms of ESDD and diameter of the contaminated insulator," *Power Engineering Review,* vol. 20, no. 9, pp. 44 - 45, 2000.

[18] P. Y. a. N. Vasudev, "Artificial Pollution Testing of Polymeric Insulators by CIGRE Round Robin Method -Withstand & Flashover Characteristics," in *Techniques in Electrical Systems*, Bangalore, 2017.

[19] A. M. a. M. T. B. Moula, "Evaluation of Insulator's Energy under Uniform Pollution Condition," *2nd IEEE ENERGYCON Conference & Exhibition,* vol. II, no. 1, pp. 1-4, 2012.

[20] M. NageswaraRao, N. Sumathi, V. Chaitanya and A. Azees, "Design of corona mitigation device and application of ZnO microvaristor on 66kV insulators by finite element method," in *IEEE International Conference on Power, Control, Signals and Instrumentation Engineering* , 2017.

[21] A. Hassanvand, H. A. Illias, H. Mokhlis and A. H. A. Bakar, "Effects of corona ring dimensions on the electric field distribution on 132 kV glass insulator," in *IEEE 8th International Power Engineering and Optimization Conference (PEOCO2014)*, 2014.

[22] P. Sidenvall, I. Gutman, L. Carlshem, J. Bartsch and R. Kleveborn, "Development of the water drop–induced corona test method for composite insulators," *IEEE Electrical Insulation Magazine,* vol. 31, no. 6, pp. 43 - 51, 2015.

[23] M. Bouhaouche, A. Mekhaldi and M. Teguar, "Improvement of electric field distribution by integrating composite insulators in a 400 kV AC double circuit line in Algeria," *IEEE Transactions on Dielectrics and Electrical Insulation,* vol. 24, no. 6, pp. 3549 - 3558, 2017.

[24] S. Ilhan, A. Ozdemir and H. Ismailoglu, "Impacts of corona rings on the insulation performance of composite polymer insulator strings," *IEEE Transactions on Dielectrics and Electrical Insulation,* vol. 22, no. 3, pp. 1605 - 1612, 2015.

[25] D. S. J. M. Seifert, "High Pollution Resistant Composite Insulators," in *Lapp Insulator GmbH & Co. KG*, Bahnhofstrasse 5 Wunsiedel, BV, 95632 GERMANY, 2008.

[26] C. L. Y. i. B. a. B. Z. Fochi Wang, "The characteristic of Concretepolluted Composite insulators," in *Key Labolatory of High Voltage and*, China, 2009.

[27] K. S. D. P. E. T. a. M. G. D. M. Dimitropoulou, "Insulation Coordination and Pollution Measurements in the Island of Crete," *IEEE International Conference on the Properties and Applications of Dielectric Materials,* no. 11, pp. 1-4, 2015.

[28] A. B. a. H. H. M. El-A. Slama, "The effect of discontinuous non uniform pollution on the flashover of polluted insulators under Lightning impulse voltage," in *International Conference on High Voltage Engineering and Application*, Shanghai, China, 2012.

[29] C. S. Y. T. X. J. L. S. W. Sima, "Flashover Performance and Voltage Correction of Iced and Polluted W Insulator String at High Altitude of 4000m and Above," *Key Laboratory of High Voltage and Electrical New Technology of Ministry of Education,* pp. 1-5, 2003.

[30] M. Teguar, D. Namane and A. Mekhaldi, "Influence of the thickness and the nature of HVAC insulator model on the flashover voltage and the leakage current," in *IEEE International Conference on Solid Dielectrics (ICSD)*, 2013.

[31] A. Vlastos and T. Sorqvist, "Leakage current and performance of silicone rubber insulators during salt-storms," in *Proceedings of 1994 IEEE International Symposium on Electrical Insulation*, 1994.

[32] L. Coffeen and J. McBride, "High voltage AC resistive current measurements using a computer based digital watts technique," *IEEE Transactions on Power Delivery,* vol. 6, no. 2, p. 19, 1991.

[33] G. S. M. I. T. S. a. M. C. Daniel Weida, "Electro-Quasistatic High-Voltage Field Simulations of Insulator Structures Covered with Thin Resistive Pollution or Nonlinear Grading Material," *Chair for Theory of Electrical Engineering and Computational Electromagnetics.*

[34] B. Almgren, B. Jacobson and D. Wu, "Long term evaluation of insulator coatings at one of the Pacific Intertie HVDC converter stations," in *Conference Record of the the 2002 IEEE International Symposium on Electrical Insulation (Cat. No.02CH37316)*, 2002.

[35] I. 6. (E), "62529-2012 - IEC 62529:2012(E) Standard for Signal and Test Definition," IEEE, 16 July 2012.

[36] S. Ilhan, A. Ozdemir, S. H. Jayaram and E. A. Cherney, "Simulations of pollution and their effects on the electrical performance of glass suspension insulators," in *Annual Report Conference on Electrical Insulation and Dielectric Phenomena*, Montreal, QC, Canada, 2012.

[37] K. Liang, J. Wang, K. Liu and L. Wang, "Research of acoustic vibration technique in online defects detection in porcelain post insulator," in *EEE International Magnetics Conference (INTERMAG)*, Beijing, China, 2015.

[38] YU Xinzhe, YANG Xiaolei, ZHANG Qiaogen, YU Xinzhe, ZHOU Jun and LIU Bo, "Effect of booster shed on ceramic post insulator pollution flashover performance improvement," in *China Electric Power Research Institute*, Beijing, China.

[39] L. L. R. H. a. L. X. Luo Bing, "Study on Pollution Flashover Characteristics of +800kV DC Composite Insulators," in *IEEE PES PowerAfrica 2007 Conference and Exposition*, Johannesburg, South Africa, 2007.

[40] M. A. B. a. M. M.A.Abouelsaad, "Environmental Pollution Effects on Insulators of Northern Egypt HV Transmission Lines," in *Annual Report Conference on Electrical Insulation and Dielectric Phenomena*, Cairo, Egypt, 2012.

[41] M. F. a. W. A. C. N. Ravelomanantsoa, "A Simulation Method for Winter Pollution Contamination of HV Insulators," in *Electrical Insulation Conference,*, Chicoutimi, CANADA, 2011.

[42] M. Raju and N. P. Subramaniam, "Comparative study on disc insulators deployed in EHV AC and HVDC transmission lines," in *International Conference on Circuit, Power and Computing Technologies (ICCPCT)*, 2016.

[43] D. Wu and D. Gustavsson, "The performance of HVDC wall bushings with silicone rubber sheds," in *IEEE Electrical Insulation Conference (EIC)*, 2015.

[44] A. Abbasi, A. Shayegani and K. Niayesh, "Pollution performance of HVDC SiR insulators at extra heavy pollution conditions," in *IEEE Transactions on Dielectrics and Electrical Insulation*, 2014.

[45] "Colombian Experience on Insulation Pollution Level Measurement Applying the ESDD Methodology," *IEEE/PES Transmission & Distribution Conference and Exposition,* pp. 1-3, 2006.

[46] "Study on the different law between NSDD and ESDD in natural environment," *Hengzhen Li ; Yunhai Song ; Gang Liu ; Yigang Liu,* pp. 1-4, 2009.

[47] F. Aouabed, A. Bayadi, S. Satta and R. Boudissa, "Conductivity effect on the flashover voltage of polluted polymeric insulator under AC voltage," *IEEE journal,* pp. 1-6, 2010.

[48] A. Abbasi, A. Shayegani and K. Niayesh, "Contribution of Design Parameters of SiR Insulators to Their DC Pollution Flashover Performance," in *IEEE Transactions on Power Delivery*, 2014.

[49] D. Huang, J. Ruan, W. Cai, T. Li, Y. Wei and J. Liu, "Flashover prevention on high-altitude HVAC transmission line insulator strings," *IEEE Transactions on Dielectrics and Electrical Insulation,* vol. 16, no. 1, p. 7, 2009.

[50] A. Karn, S. Potivejkul, N. Pattanadech and P. Yutthagowith, "Behavior comparison of corona inception and flashover voltage between HVAC and HVDC insulator," in *International Power Engineering Conference*, 2005.

[51] I. Seo, J. Koo, J. Seong, B. Lee, Y. Jeon and C. Lee, "Experimental investigation on the DC breakdown of silicone Polymer composites employable to 500kV HVDC insulator," in *1st International Conference on Electric Power Equipment - Switching Technology*, 2011.

[52] S. Taheri, M. Farzaneh and I. Fofana, "Application of dynamic two-arc model to flashover of HVDC insulators subjected to cold climate regions," in *IEEE Conference on Electrical Insulation and Dielectric Phenomena (CEIDP)*, 2015.

[53] W. Ma, B. Luo, Z. Su, Z. Dang, Z. Guan, X. Liang, U. Astrom, D. Wu, E. Long and H. Sun, "Preliminary Recommendations on the Suitable Shed Profile for HVDC Station Insulators with Silicone Rubber Housing," in *International Conference on Power System Technology*, 2006.

[54] J. M. Seifert, W. Petrusch and H. Janssen, "A comparison of the pollution performance of long rod and disc type HVDC insulators," in *IEEE Transactions on Dielectrics and Electrical Insulation*, 2007.

[55] R. Gremaud, M. Bjelogrlic, M. Schneider, E. Logakis, C. Schlegel, S. Fürsich, A. Krivda, T. Christen and U. Riechert, "Surface charge decay on HVDC insulators: Temperature and Field effects," in *IEEE International Conference on Solid Dielectrics (ICSD)*, 2013.

[56] S. Nookuea, S. Chotigo and B. Pungsiri, "A study of defective characteristics on HVAC insulators for 33 kV distribution system," in *Proceedings of 2011 International Symposium on Electrical Insulating Materials*, 2011.

[57] R. Pandian, "Leakage current and flash over performance analysis of 11 kv pin insulator under Bird excretion pollution," in *International Conference on Energy Efficient Technologies for Sustainability (ICEETS)*, Nagercoil, India, 2016.

[58] F. Aouabed, A. Bayadi, S. Satta and R. Boudissa, "Conductivity effect on the flashover voltage of polluted polymeric insulator under AC voltage," *IEEE journal,* pp. 1-6, 03 December 2010.

[59] Z. H. a. L. H. Chen Yanping, "South Africa 95 New Class 20E Locomotives," CRRC, 2013.

[60] D. Huang, W. Lu, Y. Deng, J. Ruan and Z. Xiong, "CaSO4 Content in Contamination Influence on AC Pollution Flashover Characteristics of XWP2-160 Porcelain Insulator String," in *IEEE International Conference on High Voltage Engineering and Application (ICHVE)*, ATHENS, Greece, 2018.

[61] S. Khatoon and A. A. Khan, "A comparative analysis on the performance of the contaminated conventional and composite insulators, energized by HVAC," in *International Conference on Technological Advancements in Power and Energy (TAP Energy)*, 2017.

[62] Y. Kim and K. Shong, "The Characteristics of UV Strength According to Corona Discharge From Polymer Insulators Using a UV Sensor and Optic Lens," *IEEE Transactions on Power Delivery,* vol. 23, no. 3, pp. 1579 - 1584, 2011.

[63] Z. a. Z. H. Li Hua, "South Africa 359 New Class 22E Locomotives," CRRC, 2014.

[64] X. Lu, X. Chen, D. Zhang and Z. Zhang, "Analysis on natural contamination depositing characteristics of imitative insulator string for overhead transmission line in Shantou," *Electrical Insulation and Dielectric Phenomena,* vol. 2, p. 3, 2013.

[65] L. Luo, Z. Li, Z. Hou, X. Song, J. Cui and M. Liu, "The influence factors of pin corrosion rate of disc suspension type insulators on UHVDC transmission lines," in *12th IET International Conference on AC and DC Power Transmission (ACDC 2016)*, Beijing, China, 2016.

[66] M. l. a. Manglane, "T12_6G3R5468Rev3(Spec. of PCC)," Toshiba, 2006.

[67] A. Nakagawa, "Safe operating area for 1200-V non-latch-up bipolar-mode MOSFETs".

[68] N. Okada, K. Ikeda, S. Sumi, R. Matsuoka, K. Kondo and S. Ito, "Contamination withstand voltage characteristics of hydrophobic polymer insulators under simulated rain conditions," in *Conference Record of the the 2002 IEEE International Symposium on Electrical Insulation (Cat. No.02CH37316)*, Boston, MA, USA, 2002.

[69] B. S. Reddy and A. R. Verma, "Pollution performance of HVDC insulator strings under normal and faulted conditions," in *6th IEEE Power India International Conference (PIICON)*, 2014.

[70] M. Sivaraman and J. Sivadasan, "Comparison of pollution flashover performance of various insulators," in *2014 International Conference on Circuits, Power and Computing Technologies [ICCPCT-2014]*, 2014.

Appendix A

Table A1: Properties of a polymeric insulator

Material	Relative permittivity (ε_r)	Conductivity ϭ(S/m)
Silicon	12	0
Iron Steel	14.5	0.25
Air	1	0
Dry contamination	80	0.009
Water drop	88.4	0.009
Fiberglass	5	0
Porcelain	5.9	0

Table A2: Relative resistivities of some materials at room temperature (20°C)

| Material	Resistivity, ρ (Ω.m)	Temperature coefficient of resistivity α (K^{-1})
Typical Metals		
Silver	1.62×10^{-8}	4.1×10^{-3}
Copper	1.69×10^{-8}	4.3×10^{-3}
Gold	2.35×10^{-8}	4.0×10^{-3}
Aluminium	2.75×10^{-8}	4.4×10^{-3}
Magnesium	4.82×10^{-8}	0.002×10^{-3}
Tungsten	5.25×10^{-8}	4.5×10^{-3}
Iron (Steel)	9.68×10^{-8}	6.5×10^{-3}
Platinum	10.6×10^{-8}	3.9×10^{-3}
Typical Semiconductors		
Silicon, pure	2.5×10^3	-70×10^{-3}
Silicon, *n*-type	8.7×10^{-4}	-
Silicon, *p*-type	2.8×10^{-3}	-
Typical Insulators		
Glass	$10^{10} - 10^{14}$	-
Fused quartz	10^{16}	-
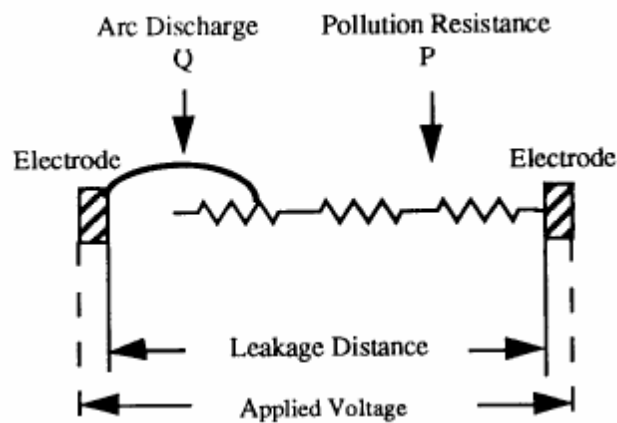
Figure 45: Obenaus model of polluted insulator [5]

Appendix B

Table B3:U70BS Glass insulator requirements standards of IEC 60383-1 (ball and socket coupling)

Sample no	Disc diameter 260±12 mm	Spacing 138±4.5 mm	Creepage distance 325±8.7 mm	Ball and socket coupling
1	259.5	137.0	320	Ok
2	258.9	138.5	320	Ok
3	258.4	137.0	317	Ok
4	258.0	137.0	320	Ok
5	258.0	138.2	322	Ok

Table B4: Glass and Porcelain insulator thickness and quality of coupling zinc coating requirements standards of IEC 60383-1

Sample no	Thickness of zinc coating (μm)	
	Pin	Cap
	Average value	Average value
1	108	127
2	120	136
3	110	213
4	142	122
5	110	182

Table B5: Glass and Porcelain insulator of the radio interference requirements standards of IEC 60383-1

U_{50} (kV)	Y_n (dB)	K (dB)	Y_i (dB)
40	106	17	123
35	76		93
30	58		75
25	47		64
20	32		49
15	9		29
10	2		19

Table B6: Porcelain and glass insulators of the lighting impulse withstand voltage test requirements standards of IEC 60383-1

Sample no	Polarity	Number of impulses applied	Tested withstand voltage, kV	Corrected withstand voltage, kV	Test voltage, kV	Test Results
1	Positive	15	110	107.4	118.3	Withstood
1	Negative	15	115	112.3	123.7	Withstood
2	Positive	15	110	107.4	118.1	Withstood
2	Negative	15	115	112.2	123.6	Withstood
3	Positive	15	110	107.4	118.5	Withstood
3	Negative	15	115	112.2	123.6	Withstood
4	Positive	15	110	107.4	118.4	Withstood
4	Negative	15	115	112.2	123.5	Withstood
5	Positive	15	110	107.4	118.3	Withstood
5	Negative	15	115	112.2	123.7	Withstood

Table B7: Porcelain and glass insulators of a wet power frequency withstand voltage tests standards of IEC 60383-1

Sample no	Tested withstand voltage, kV	Test voltage, kV	Corrected tested withstand voltage, kV	Duration of voltage application, s	Result
1	45	41	41.1	60	Not withstood
2	45	40	40.1	60	Not withstood
3	45	42	42.1	60	Not withstood
4	45	40	40.1	60	Not withstood
5	45	40	40.1	60	Not withstood

Table 8: Flashover results of the polymeric, porcelain and glass insulator Under Positive DC Voltage.

Flashover voltage (kV)	Conductivity ϭ(S/m)		
	Polymeric Insulator	Porcelain Insulator	Glass Insulator
55	0.17	0.12	0.13
70	1.23	1.1	1.14
85	2.21	2.01	2.09
100	3.56	3.2	3
115	4.78	4.42	4.24
130	5.66	5.21	5.50

Table B9: Leakage Currents for a clean Porcelain, Glass and Polymeric insulators under HVAC

AC voltage (kV)	Porcelain insulator Leakage current (μA)	Glass insulator Leakage current (μA)	Polymeric insulator Leakage current (μA)
10	113.10	94.25	37.70
20	226.20	188.5	75.40
30	339.30	282.75	113.10
40	452.40	377.00	150.80
50	565.50	471.25	188.50
60	678.60	565.50	226.20
70	791.70	656.75	263.90
80	904.80	754.00	301.60
90	1017.90	848.25	339.30
100	1131.00	942.50	377.00
110	1244.10	1036.75	414.70
120	1357.20	1131.00	452.40
130	1470.30	1225.25	490.10
140	1583.40	1319.50	527.80

Table B10: Leakage Currents for dry contaminated Porcelain, Glass and Polymeric insulators under HVAC

AC voltage (kV)	Porcelain insulator Leakage current (mA)	Glass insulator Leakage current (mA)	Polymeric insulator Leakage current (mA)
10	0.90	0.66	0.58
20	1.22	0.70	0.87
30	1.60	1.07	1.29
40	2.50	1.02	1.54
50	3.03	1.09	1.66
60	3.20	1.25	2.31
70	4.33	1.55	1.98
80	6.05	3.21	2.97
90	8.05	4.78	3.98
100	9.66	6.29	5.96
110	10.30	9.66	8.87
120	12.10	9.87	9.56
130	13.20	11.32	10.10
140	13.70	12.50	11.02
150	14.50	13.01	11.76
160	14.80	13.89	12.90

Table B11: Leakage Currents for wet contaminated Porcelain, Glass and Polymeric insulators under HVAC

| AC voltage (kV)	Porcelain insulator Leakage current (µA)	Glass insulator Leakage current (µA)	Polymeric insulator Leakage current (µA)
10	103.7	84.5	40.7
20	206.5	168.5	86.4
30	309.4	262.5	114.1
40	432.2	357.5	160.8
50	546.0	451.5	198.5
60	658.6	545.5	236.3
70	771.7	636.0	273.5
80	884.6	724.9	310.6
90	974.0	824.5	349.3
100	1111.0	922.5	387.0
110	1200.5	1016.5	424.3
120	1337.1	1111.0	462.2
130	1450.3	1200.5	501.1
140	1563.4	1300.5	537.3
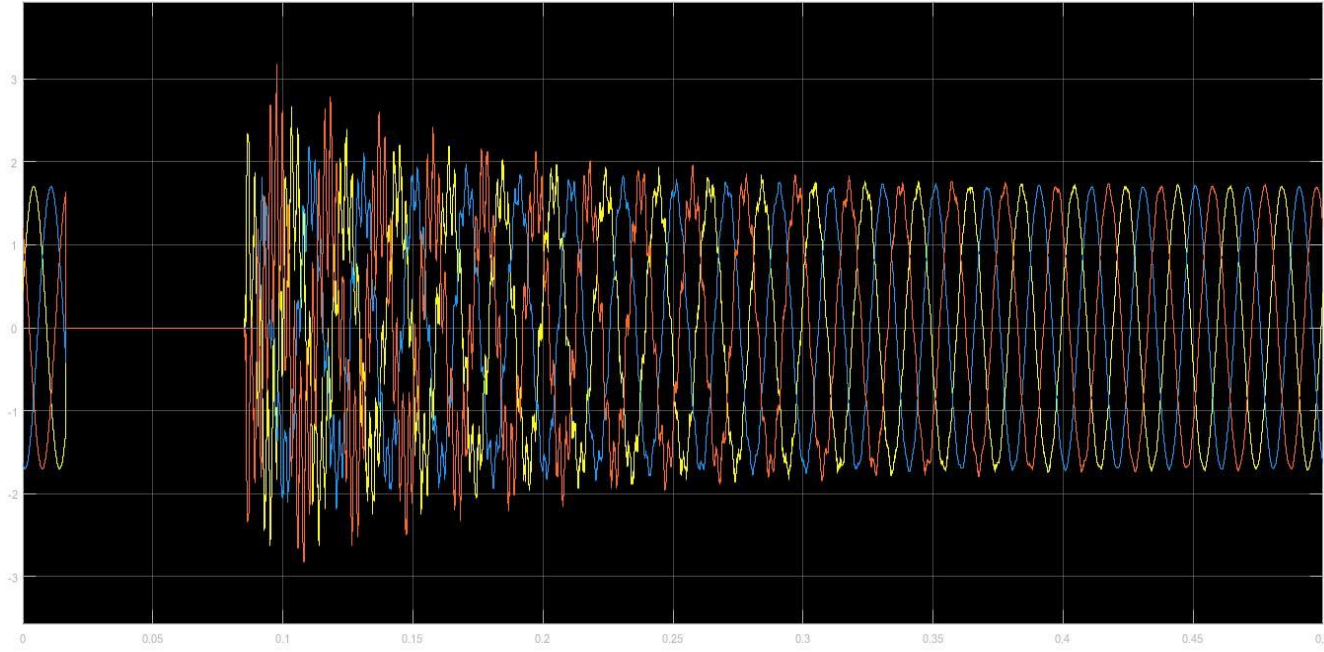
*Figure B46: Flashover voltage detection of a HVAC three-phase line*
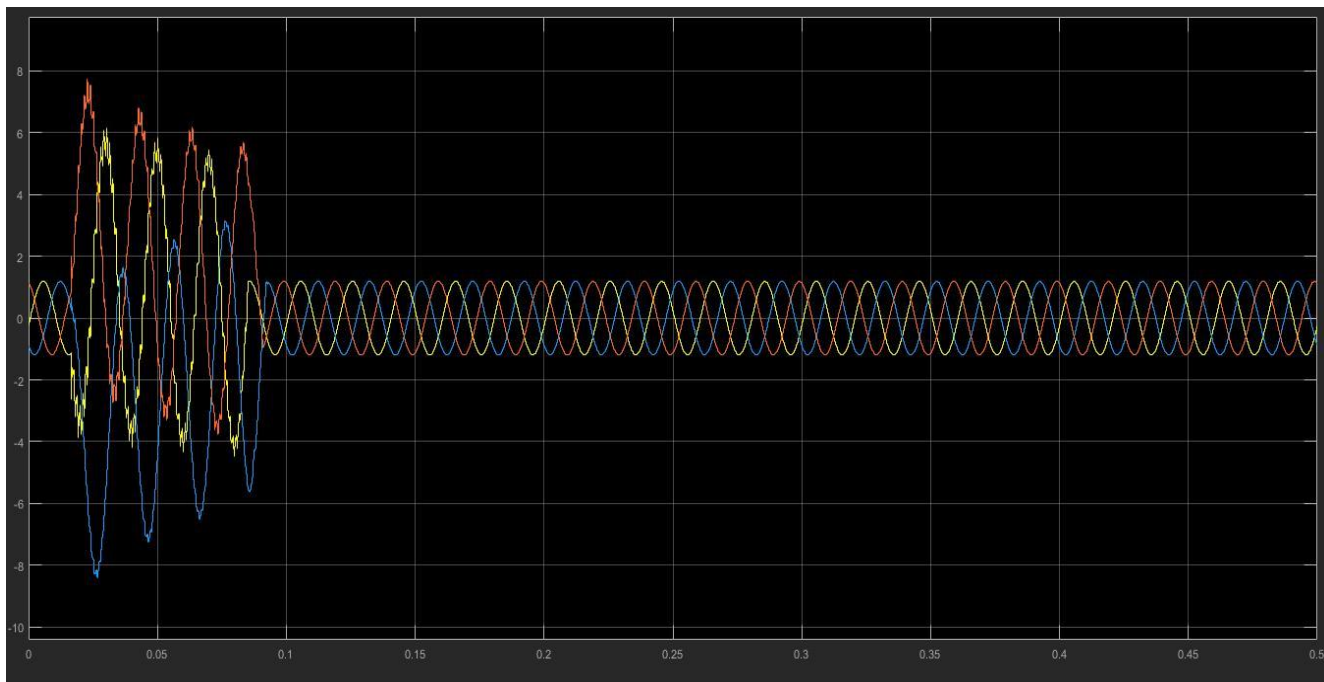
*Figure B47: Flashover current detection of a HVAC three-phase line*
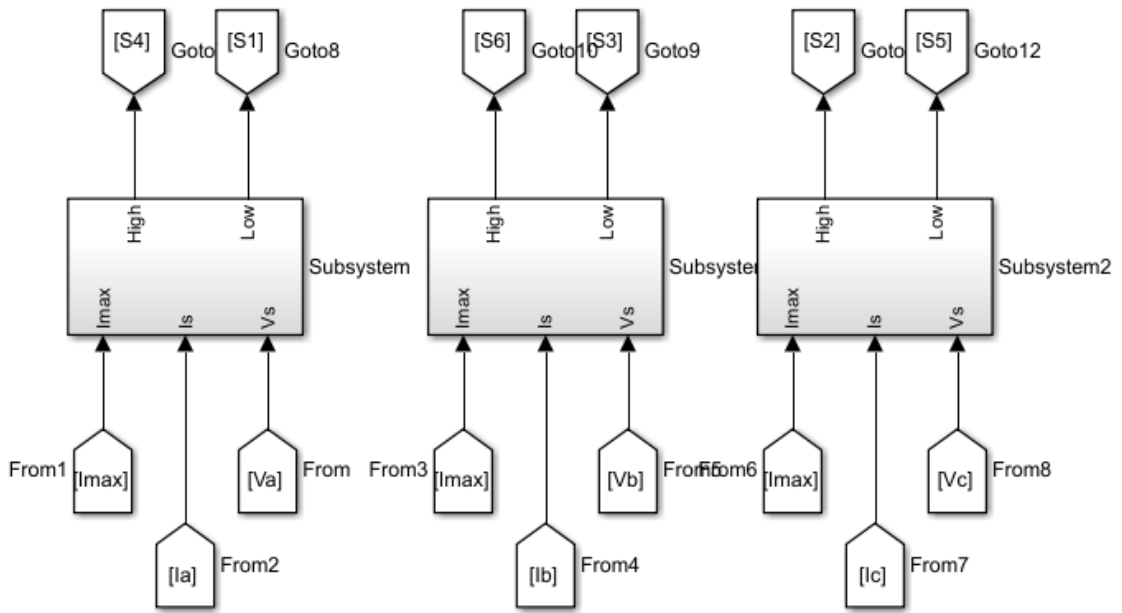
Figure B48: Control subsystem
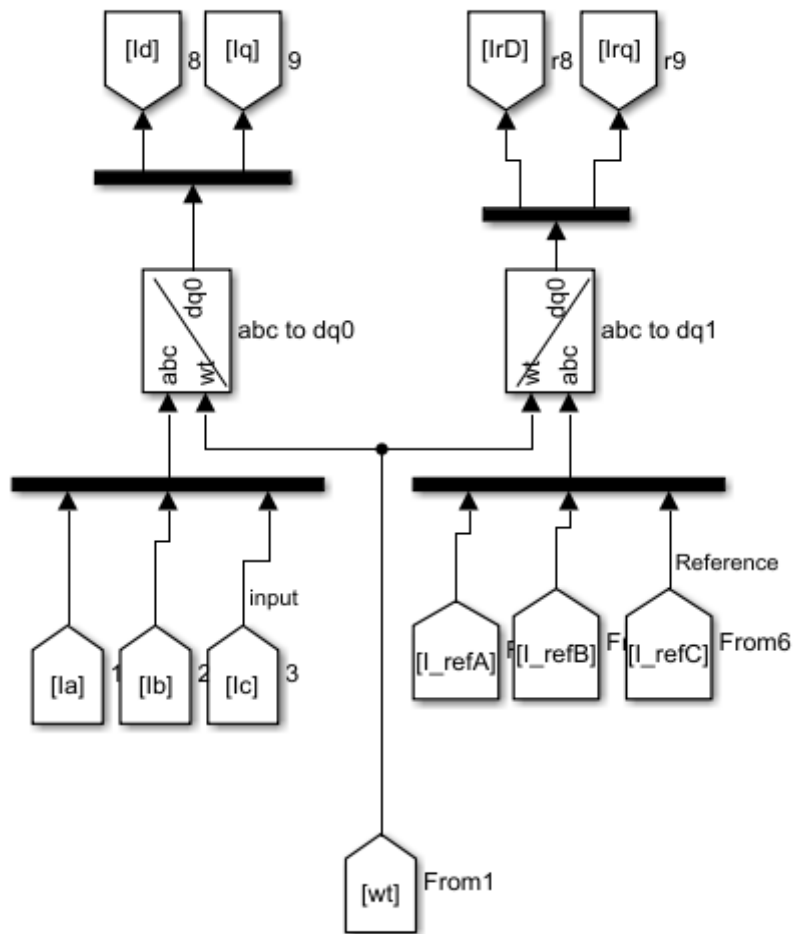

Figure B49: Control function of the subsystem
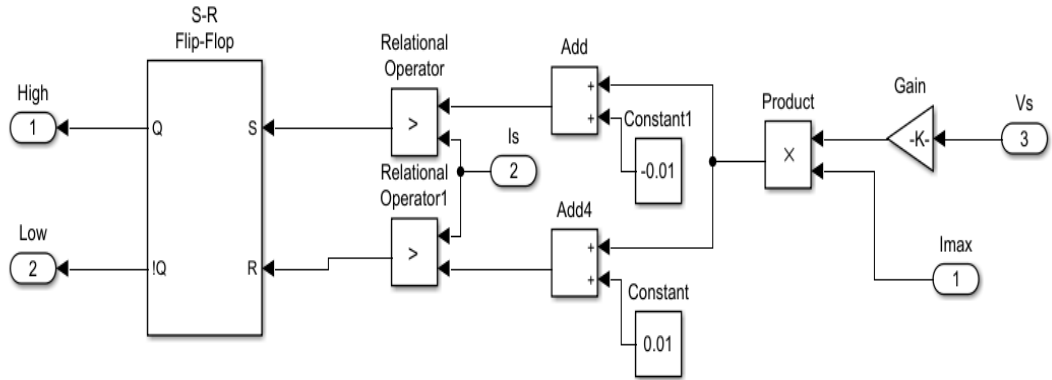
Figure B50: Logic function of the subsystem
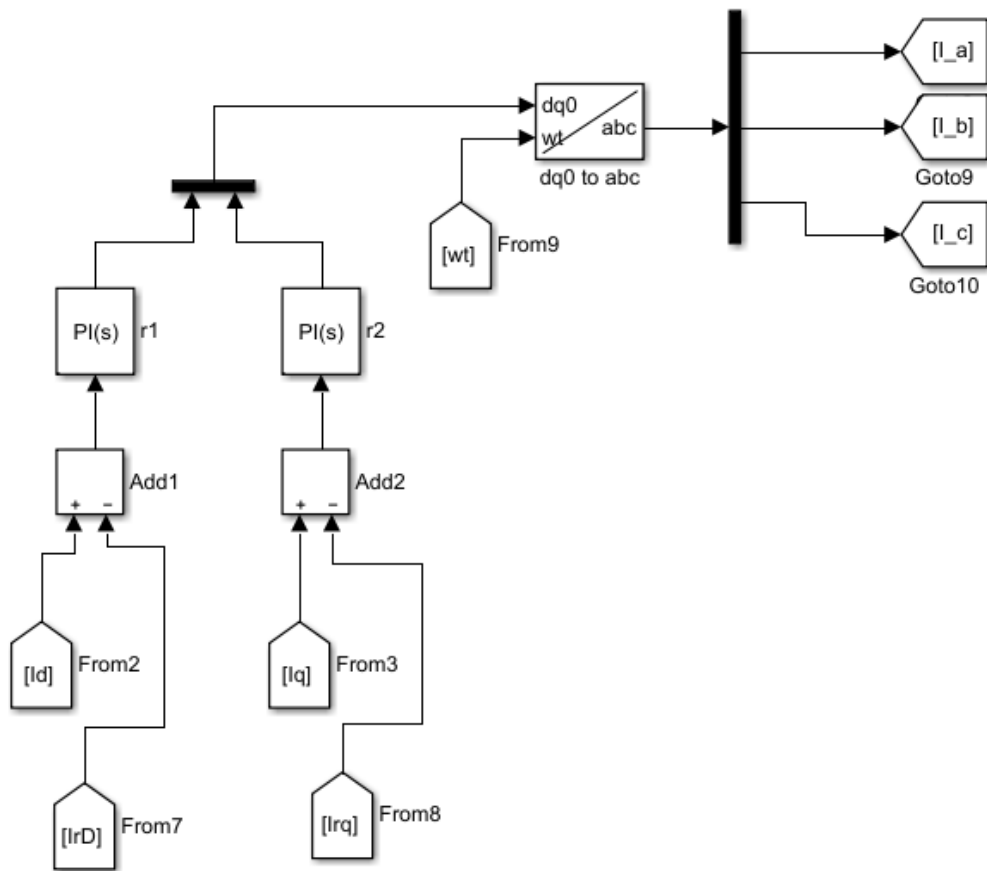
Figure B51: Feedback function of the subsystem

Table B12: Leakage Currents for dry contaminated Porcelain, Glass and Polymeric insulators under HVDC

HVDC Voltage (kV)	Leakage current (μA)		
	Porcelain insulator	Glass Insulator	Polymeric insulator
10	0.1732	0.1918	0.6000
20	0.3534	0.4196	1.9568
30	0.4982	0.6258	3.2354
40	0.6975	0.8246	7.0350
50	0.9744	1.4587	13.759
60	1.2531	4.1682	21.405
70	1.3892	7.3254	34.569
80	1.5783	10.523	55.217
90	1.6438	13.135	81.362
100	3.7986	17.019	107.03
110	4.2534	21.684	139.65
120	5.7382	26.031	174.90
130	7.2314	31.529	195.21
140	9.7105	39.850	228.26
150	21.639	59.562	256.58
160	34.025	80.713	311.54
170	62.654	152.38	346.94
180	93.658	192.94	382.59

Table B13: Leakage Currents for wet contaminated Porcelain, Glass and Polymeric insulators under HVDC

HVDC Voltage (kV)	Leakage current (μA)		
	Porcelain insulator	Glass Insulator	Polymeric insulator
10	9.2565	11.357	3.2995
20	26.843	34.477	7.5689
30	54.269	68.652	9.8546
40	94.587	109.85	10.997
50	121.63	135.29	13.215
60	187.54	196.11	15.687
70	211.45	233.78	18.987
80	258.92	242.11	27.231
90	298.56	259.94	31.594
100	321.89	274.13	39.329
110	354.20	298.56	51.263
120	374.57	325.49	67.338
130	409.86	352.06	79.256
140	448.33	378.97	91.235
150	481.22	417.04	101.66
160	501.26	501.26	124.03
170	512.67	512.67	142.93
180	547.92	547.92	151.72

Table B14: Alternating current systems in use in the world for electric locomotives

AC voltage and frequency	Countries
11kV - 16²/3 Hz	Switzerland
15kV - 16²/3 Hz	Austria, Germany, Norway, Sweden, Switzerland
6,5kV - 25 Hz	Austria
11kV - 95 Hz	USA
20kV - 50 Hz	Japan
25kV - 50 Hz	Bulgaria, China, Czechoslovakia, Denmark, Finland, France, Germany, Great Britain, Hungary, India, Japan, Luxembourg, Pakistan, Portugal, Romania, South Africa, Turkey, Yugoslavia, Zaire, Zimbabwe, Australia, USA
50kV - 50 Hz	USA, South Africa
20kV - 60 Hz	Japan
25kV - 60 Hz	Japan, South Korea
50kV - 60 Hz	USA, Canada

Table B15:Table B12: Alternating current systems in use in the world for electric locomotives

DC voltage	Countries
630/750/1200V	Great Britain, USA, Canada
1500V	Australia, Czechoslovakia, Denmark, France, Great Britain, Holland, India, Japan, New Zealand, Portugal, Spain, USA, Egypt
3000V	Algeria, Belgium, Chile, Czechoslovakia, Italy, Luxembourg, Morocco, Poland, South Africa, Spain, USA, Yugoslavia

Table B16 Locomotive operation voltages

Electrification system	Lowest non-permanent voltage U_{min2} (V)	Lowest non-permanent voltage U_{min1} (V)	Nominal voltage U_n (V)	Highest non-permanent voltage U_{max1} (V)	Highest non-permanent voltage U_{max2} (V)
DC (mean values)		400 500 1000 2000	600 750 1500 3000	720 900 1800 3600	770 950 1950 3900
AC (rms values)	11000 17500	12000 19000	15000 25000	17250 27500	18000 29000